STRUCTURE - PROPERTY RELATIONSHIP IN VOLCANIC ASH BASED ONE PART GEOPOLYMERS AND PERLITE-METAKAOLIN BASED TWO PART GEOPOLYMERS

by

Refika Çetintaş

B.S., Biological Sciences, Middle East Technical University, 2011

B.S., Chemical Engineering, Middle East Technical University, 2012

Submitted to the Institute for Graduate Studies in
Science and Engineering in partial fulfillment of
the requirements for the degree of
Master of Science

Graduate Program in Chemical Engineering

Boğaziçi University

2018

To my husband

ACKNOWLEDGEMENTS

First and foremost, I would like to thank my supervisor, Assoc. Prof. Sezen Soyer Uzun, for not only providing me the opportunity to work with her but also being a great mentor. I am grateful for writing my thesis under her guidance and with her support, encouragement and geniality at all levels of my research.

I would also like to express my gratitude to Assoc. Prof. Alper Uzun and Samira F. Kurtoğlu who have been so helpful and cooperative in giving their support at all times to help me to achieve my goal. I am particularly grateful to Samira F. Kurtoğlu for her assistance in XRD, FTIR and SEM analysis.

I also appreciate Assoc. Prof. Nilüfer Özyurt Zihnioğlu and Abdullah H. Akça for their technical assistance and patience during compressive strength measurements.

I would also like to thank my colleagues: Ramazan Oğuz Canıaz, Emel Başkent, Elif Kocaman, Serhat Arca and Kardelen Kaya for their help during my research.

I would like to express my deep gratefulness to my family for their love and support. They are the biggest source of my strength. They have made tremendous contributions to me to reach this stage in my life.

I would like to dedicate this thesis to my husband, my dearest, Osman Oğuz Çetintaş. I thank him for putting up with me in difficult moments and for encouraging me to get this degree. This would not be possible without his unwavering and endless love and support. I thank him with all my heart for always standing by me.

This work was supported by Bogazici University Research Fund through Project BAP 17A05P1.

ABSTRACT

STRUCTURE - PROPERTY RELATIONSHIP IN VOLCANIC ASH BASED ONE PART GEOPOLYMERS AND PERLITE-METAKAOLIN BASED TWO PART GEOPOLYMERS

In this thesis, structure-property relations in volcanic ash and perlite-metakaolin based geopolymer systems are investigated. In the first part of the thesis, volcanic ash is used as raw material to synthesize *one-part* (just add water) geopolymers using anhydrous sodium metasilicate particles as the sole alkaline activator. Volcanic ash based *one-part* geopolymers are synthesized at ambient temperature with varying molar Si/Al (2.5-4.5) and Na/Al (1.1-5.1) ratios with a constant water/solid (wt/wt) ratio of 0.3. The geopolymers are comprised of X-ray amorphous phases and some undissolved crystalline phases (aluminosilicate and iron oxide phases) embedded in the amorphous matrices. The main absorption band in the FTIR spectra assigned to the asymmetric stretching vibrations of Si-O-T (T: Si, Al) shifts to lower frequencies with increasing Si/Al molar ratio, which is a significant indication of the formation of amorphous aluminosilicate gel phase. The corresponding compressive strength values of *one–part* geopolymers ascend from 13.89 MPa to 19.60 MPa as the SEM morphologies of the specimens display denser, smoother and more homogenized glassy matrices. In the second part of the thesis, perlite-metakaolin based foamed geopolymers are synthesized with varying metakaolin contents of 0, 10, 20, 30, 40, 50, 100 wt% in raw material. The specimens are foamed by means of 3 wt% hydrogen peroxide. XRD patterns depict that the halo peak centered at around 23°shifts to the higher angles (~27-29° 2θ) as Si/Al molar ratio decreases, which is indication of polymerization. Zeolite crystalline phases are remarkable for geopolymers including 20 wt% and higher proportions of metakaolin, consistent with the corresponding SEM micrographs. As water/solid ratio increases, total pore volume of geopolymers increases leading to a decreasing trend in density of the geopolymers. The lowest density achieved in this study is 1.74 g/cm^3. Thermal gravimetric analysis indicates that the lowest thermal stability is attained for sample with the highest total pore volume.

ÖZET

VOLKANİK CÜRUF BAZLI TEK AŞAMALI JEOPOLİMERLERİN VE PERLİT-METAKAOLİN BAZLI İKİ AŞAMALI JEOPOLİMERLERİN YAPI - ÖZELLİK İLİŞKİSİ

Bu tezde, volkanik cüruf ve perlit-metakaolin bazlı jeopolimerlerin yapı-özellik ilişkileri incelenmiştir. Tezin ilk bölümünde, alüminosilikat ham maddesi olarak volkanik cüruf ve alkalin aktivatör olarak susuz sodyum metasilikat tek aşamalı jeopolimerlerin sentezlenmesinde kullanılmıştır. Değişen Si/Al (2.5-4.5) ve Na/Al (1.1-5.1) mol oranları ile sabit su/katı 0.3 (ağ./ağ.) oranında volkanik cüruf bazlı tek aşamalı jeopolimerler oda koşullarında sentezlenmiştir. Jeopolimerler, X-ray amorf yapıdadır ve bazı çözünmemiş kristal fazlar (alüminosilikat ve demir oksit fazları) da amorf yapıda bulunmaktadır. FTIR spektralarında Si-O-T (T: Si, Al) asimetrik gerilimine atfedilen ana bant, Si/Al mol oranı arttıkça daha düşük frekanslara kaymaktadır ve bu durum amorf alüminosilikat jel yapısının oluştuğunun belirgin göstergesidir. Örneklerin SEM morfolojileri daha yoğun ve homojen camsı yapı sergiledikçe, tek aşamalı jeopolimerlerin basınç dayanımları 13.89 MPa'dan 19.60 MPa'ya artmaktadır. Tezin ikinci bölümünde perlit ve metakaolin bazlı köpürtülmüş jeopolimerler ağırlıkça 0, 10, 20, 30, 40, 50, 100 oranlarında metakaolin içerecek şekilde sentezlenmiştir. Numuneler %3 (ağ.) hidrojen peroksit ile köpürtülmüştür. XRD kırınım görüntüleri göstermektedir ki 23° civarında merkezlenmiş halo pik, Si/Al mol oranı azaldıkça daha yüksek açılara (~27-29° 2θ) kaymaktadır ve bu durum polimerleşmenin göstergesidir. %20 (ağ.) ve üzerinde oranlarda metakaolin içeren jeopolimerlerde kristal zeolit fazlarının oluşumu dikkat çekmektedir ve bu oluşumlar SEM görüntüleri ile uyumludur. Sıvı/katı (ağ./ağ.) oranı arttıkça, toplam gözenek hacmi artmakta ve jeopolimerlerin yoğunlukları azalmaktadır. Bu çalışmada elde edilen en düşük yoğunluk değeri 1.74 g/cm^3'tür. Termogravimetrik analiz, en düşük ısıl stabilitenin en yüksek gözenek hacmine sahip örnekte olduğunu göstermiştir.

TABLE of CONTENTS

LIST OF FIGURES

LIST OF TABLES

LIST OF ACRONYMS/ABBREVIATIONS

AAC	Autoclaved Aerated Concrete
BET	Brunauer-Emmett-Teller
BJH	Barrett-Joyner-Halenda
DSC	Differential Scanning Calorimetry
EDX	Energy Dispersive X-ray
FTIR	Fourier Transform Infrared Spectroscopy
OPC	Ordinary Portland Cement
SEM	Scanning Electron Microscopy
TG	Termogravimetry
TGA	Thermogravimetric analysis
Wt	Weight
XRD	X-ray Diffraction

1. INTRODUCTION

Ordinary Portland Cement (OPC) is used in the production of concrete, which is the most widely used building material in the world since 1800s. The consumption of concrete among any kind of materials has the second place just behind water [1]. Since the consumption of OPC based concrete is so tremendous, the sustainability of it should be questioned. There are two main parameters affecting the sustainability of the OPC based infrastructures: material greenness and durability [2]. Material greenness is determined according to the following three parameters: consumption of virgin resources, production of pollutants during the process and embodied energy meaning that energy consumed during production, transportation etc. [2]. In order to increase the material greenness of OPC, the production of CO_2 and energy consumption should be reduced. However, the CO_2 release is inevitable during production process and almost 1 ton of CO_2 is emitted during the production of 1 ton of cement as a direct result of calcination of limestone and silica at high temperatures [3]. It is pointed out that cement industry produces substantial amount of CO_2 and this leads to approximately 5-8% of worldwide CO_2 emissions [4]. Besides CO_2 emissions, the cement industry consumes high amount of energy corresponding to 5% of global industrial energy consumption [5]. The next sustainability parameter is durability and it refers to the service life of material. The durability of OPC is highly limited due to its brittle nature and this leads to cracking under any mechanical and environmental loading [2]. Since material greenness and durability, namely, sustainability of OPC is not so high, researchers have focused on alternative materials for OPC and geopolymer is one of the potential candidates.

The term “geopolymer” was coined by Joseph Davidovits in the late 1970’s. The geopolymers (or inorganic polymers) are synthesized by the alkali activation of aluminosilicate materials. Combination of energy efficient manufacturing process with the correct mix design and formulation will provide to produce sustainable materials with specific properties to be used in different application areas (building industry, refractories or encapsulation of wastes etc.) at a competitive cost [6, 7].

1.1. Raw Materials

The geopolymers could be synthesized from any material containing silica and alumina bearing phases. Both aluminosilicate waste materials (fly ash, red mud, coal ash, blast furnace slag, volcanic ash etc.) and natural sources (metakaolin, perlite or other clays) can be utilized in the formation of geopolymers [6, 7, 8].

Volcanic ashes contain high amount of alumina and silica (see Table 1.1) and this makes them one of the potential candidates for geopolymer synthesis [9]. Volcanic eruptions are frequently seen in different parts of the world and this causes accumulation of huge volcanic ash deposits at the surface [10, 11]. These deposits are easily accessible for mining and being at the surface has the advantage of not only low cost mining but also minimum negative environmental effect [12, 13]. Besides, the production of volcanic ash based geopolymers could have economic importance for the countries possessing high amounts of volcanic ash deposits with past or present volcanism [12]. Volcanic ashes are used as an additive in the production of Portland cement in some countries [10] but utilizing them in the production of long term durable geopolymers would be a great alternative for Portland cement and construction industry. Nevertheless, there are limited researches on volcanic ash based geopolymers even in the countries with huge deposits [14]. In Turkey, there are large amounts of volcanic ash deposits in the west and some parts of the Mediterranean region but there are no research about the geopolymerization of these volcanic ashes.

Perlite, glassy aluminosilicate, is a natural source that can be used in geopolymer synthesis. The chemical composition of perlite is tabulated in Table 1.1, and the percentages of SiO_2 and Al_2O_3 ranges between 70–75 and 12–18, respectively [15]. Perlite has 2-5 % (wt.) combined water and this property provides volume expansion (4-20 times of its initial volume) and porous structure when the material is heated to 760–1100 °C [16, 17, 18]. This heated material is called as expanded perlite which has lower bulk density (80-240 kg/m^3) due to volatilization of combined water during heating, when compared to the unexpanded perlite [16, 19]. Expanded perlite is used in construction industry as insulation material or lightweight aggregate due to its lower bulk density.

The fact that heating process means consumption of high energy, utilizing the perlite as it is mined (or unexpanded perlite) in geopolymerization would be more efficient. Low-cost open-pit mining methods are used for the exploitation of perlite deposits and the known perlite reserve in the world is ~7 billion tones and more than half of these perlite reserves are located in Turkey [15, 20, 21, 22]. According to the U.S. Geological Survey report in 2016 [23], the annual production of perlite is around 2.680.000 mtons in the world and in that year the annual production of perlite is 1.100.000 mtons and 700.000 mtons in Turkey and Greece, respectively. The numbers manifest that Turkey and Greece are the world's leading perlite producers. Such a high amount of production rates can be converted to more valuable and greener products to be used in many different application areas.

Table 1.1. Chemical composition of volcanic ash, perlite and metakaolin from domestic sources [24, 15, 25]

Component %	**Volcanic Ash**	**Perlite**	**Metakaolin**
SiO_2	41.22	71.1	56.2
Al_2O_3	16.05	13.0	41.0
CaO	10.33	1.6	0.09
Fe_2O_3	7.84	1.6	0.36
MgO	6.43	0.5	0.07
Na_2O	4.29	4.2	-
K_2O	3.00	3.8	0.46
SO_3	0.37	1.6	-
TiO_2	-	-	1.15

Metakaolin is an anhydrous aluminosilicate that is obtained by the calcination of kaolin at high temperatures (650-750 °C) and during the calcination process octahedrally coordinated aluminum layers transforms into the more reactive tetrahedral forms [26, 27]. When the water molecules between Al and Si layers in kaolin are removed, relatively ordered structure arranged by silica and alumina layers is formed and this material is named as metakaolin. Metakaolin is highly reactive metastable clay and to take the advantage of this property, it was used in cement mixtures to initiate reactions between metakaolin and calcium hydroxide formed during hydration reactions [27].

Metakaolin is mostly used raw material in geopolymer synthesis due to the fact that it contains high ratio of SiO_2 and Al_2O_3, and merely of other oxides (See Table 1.1.). According to the report published by Republic of Turkey Ministry of Economy in 2017, estimated kaolin reserves in Turkey are about 100 million tons [28] and it is stated in the U.S. Geological Survey report that Turkey kaolin production is 2.000.000 mtons in 2016 [29].

1.2. Geopolymerization Process and Method of Synthesis

Geopolymer, which "geo" refers to inorganic aluminosilicate materials based on geological materials, defines a polymeric silicon-oxygen-aluminum framework structure [30, 31]. In this 3-D silicon-oxygen-aluminum framework, all oxygen atoms are shared by SiO_4 and AlO_4 tetrahedral units.

The exact mechanism of geopolymerization reaction is not known in depth [32] but it is agreed that geopolymers are synthesized by multistep simultaneous reactions [30]. First of all, Al and Si species in raw material dissolve in highly alkaline environment and then active surface groups and soluble species polymerize to constitute gel structure. In the final step, this gel structure hardens to form rigid solid [33, 34]. The type of alkaline source and aluminosilicate raw material affect the chemistry and degree of alkalination but the mechanism of geopolymerization do not depend on the starting materials [30]. Reaction mechanism of geopolymerization process is presented below:

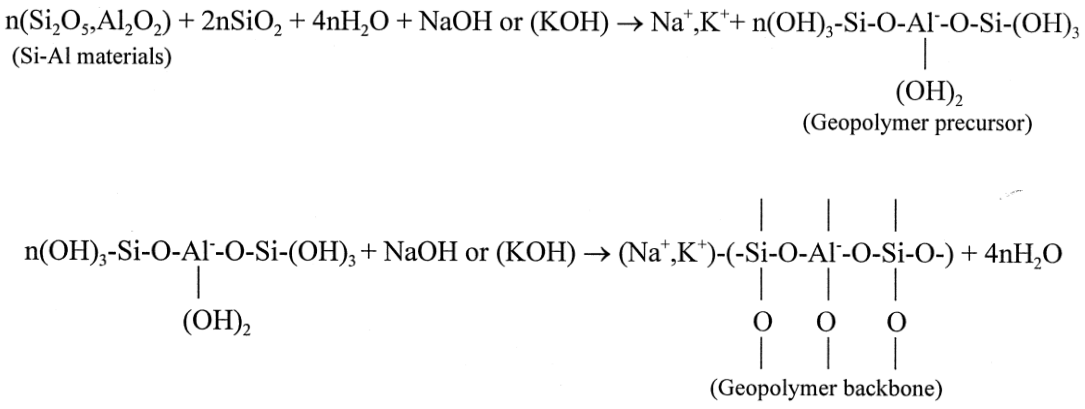

Figure 1.1. Schematical representation of geopolymer reaction from aluminosilicate sources [35]

As illustrated in Figure 1.1., Si-O-Si and Si-O-Al covalent bonds are broken by the hydroxyl ions in alkaline environment and after that Al and Si species are released. These species interact with each other and leads to formation of oligomers (dimer, trimer). Particle size and structure of raw material, molarity of alkaline solutions affect the dissolution rate of aluminosilicates [30, 32]. These oligomers lead to intermediate product with high Al content that turns into Si content rich phase. Finally, growing of gel structures lead to the formation of 3-D macromolecular structures and this process is very rapid. It is hard to designate each reaction step in details because of the fact that multistep reactions occur at the same time and the kinetics of the reactions is dependent to each other [30, 36].

There are two types of method of synthesis for geopolymers and these methods are referred as “two-part mix (conventional method)” and “one-part mix (or just add water)”. In the first method, solid aluminosilicate material and alkaline solution are used to initiate geopolymerization reaction. There are lots of disadvantageous of this conventional synthesis method; for instance, the alkaline solutions are viscous and highly corrosive which cause handling problems in commercial scale applications [37, 38]. Besides, the formation of sticky and thick paste complicates to control the rheology of geopolymer especially when the alkali source is sodium [38]. Next, if aluminosilicate raw material is utilized as silica source in geopolymerization reaction, it is quite difficult to manage the ratio of alkali to available silicate which is a critical parameter in geopolymer systems [39, 40]. Another drawback of the “two-part mix” is that if the alkali and water content is not attentively controlled, absorption of water or efflorescence problems might come out in curing period or in use [40, 41]. Latter method, “one-part mix” is more convenient to large scale applications due to those drawbacks of the conventional synthesis method. In the “one-part mix” method of synthesis, solid silicates are used as activators instead of activator solutions and water is added to dry mixture of solid aluminosilicate and solid silicates, which is quite similar to the preparation of Portland-cement [42, 43]. These advantageous make this method more attractive for the researchers and some reports indicate that compressive strengths of one-part geopolymers are comparable to two-part geopolymers [42, 44]. Researchers point out that since it is difficult to reach high alkalinity with powdered solid activator at initial dissolution step, utilization of the easily leachable aluminosilicate raw materials would be more appropriate for one-part geopolymerization [45, 46].

1.3. Properties and Application Areas of Geopolymers

The nature of initial raw materials used in geopolymerization directly affects the microstructure and properties of the final products but the macroscopic properties are similar because of the fact that silicon-aluminum bonding is same in geopolymers [32]. High compressive strength, lightweight, high resistance to any thermal and chemical attack are exhibited by the geopolymers and these excellent physical and mechanical properties provides wide application areas to geopolymers [30].

Compressive strength of geopolymers can reach to 20 MPa after 4 hours curing at ambient temperatures and 70-100 MPa can be achieved after 28-day [47]. The geopolymers can achieve high compressive strengths as long as the dissolution rate of aluminosilicate source is high and it is easily dissolved because one of the most critical parameter in geopolymerization is the amount of aluminosilicate species in the medium [30]. Duxson *et al.* [32] state the other parameters that influence the compressive strength of geopolymers as amorphous nature of raw materials, amount of gel phase formed and strength of it.

Lightweight is another property that geopolymers possess and related with the bulk density of the geopolymer. Lightweight geopolymers has lower bulk density compared to the Portland cement and this characteristic assures various application areas in building industry. Curing condition is the main affecting parameter bulk density of geopolymers and as curing temperature rises, the bulk density decreases [48]. Beside to curing temperature, concentration of alkali solution, aluminosilicate raw material and type of alkali activators are other parameters affecting bulk density. For instance, K-based geopolymers are denser than Na-based geopolymers [30, 49].

Geopolymers have high thermal stability (up to 1000-1200 °C) and exhibit low shrinkage after drying meaning that formation of cracks is prevented [50, 51]. Fillers or foaming agents can be added to the geopolymer mixture to increase their thermal properties and enhance their application areas. For instance, foamed geopolymers with low density are potential candidates as thermal insulators and geopolymers with low thermal conductivity and resistance are suitable for fire resistance applications [30, 52].

Geopolymers are also utilized in encapsulation (or immobilization) of toxic wastes because of the fact that they have high resistance to leaching in acidic and alkaline media [53, 54]. Low cost and high flexibility are other properties of geopolymers that draw attention of researchers to be used them in immobilization of heavy metals and radioactive wastes [55]. Elements in hazardous wastes (e.g. mercury, lead) are immobilized by locking them into the 3-D geopolymer network and this provides conversion of semi-solid waste into an adhesive solid [56] . This kind of incorporation is affected by two parameters: ionic size and valence of a specific ion; and ionic size and immobilization efficiency are directly correlated [57].

The unique properties of geopolymers, which depend on the mixture design and curing technique, make the geopolymerization promising technology for new construction materials [58]. There are pilot scale studies for the application of geopolymers and some of them are applied in commercial scale [50, 58]. For example, GEOPOLYMITE® and PYRAMENT® blended cement are used in thermal insulation of buildings and for the production of precast concrete, respectively [59]. Besides, to prevent cabin fire in the case of accidents, aviation industry has used fireproof fiber reinforced geopolymer composites since 1994. Since geopolymers are resistant to heat, fire and corrosion, they are also used by Formula One teams [60].

1.4. Factors Affecting Properties of Geopolymers

Alkali concentration, solid/liquid ratio, alkali reactant ratio, molar ratios, water content and curing conditions are the main affecting factors of final properties of geopolymer products. To begin with, physical and mechanical properties of the geopolymers are highly influenced by alkali concentration. Some of the researchers claim that increasing alkali concentration provides development of compressive strength due to the fact that if the alkali concentration is low, OH^- and Na^+ will not be sufficient for the dissolution of aluminosilicates and completion of geopolymerization, respectively [61]. On the other hand, other researchers argue that there is an optimum value for alkali concentration and if that optimum value is exceeded, the strength of geopolymers is negatively affected since dissolution of aluminosilicate raw material is prevented in highly viscous medium [30].

The ratio of solid aluminosilicates to alkali solution, the next factor, has effects on dissolution rate and workability. If solid/liquid ratio is high, the workability of geopolymers decreases because of low viscosity of the medium; if this ratio is low, geopolymerization period increases [62] and high compressive strength is not attained [63]. Thus, the optimum value is needed for solid/liquid ratio as in the case of alkali concentration. Beside to these factors, the alkali reactant ratio (e.g. Na_2SiO_3/ NaOH) is also crucial for the strength of geopolymers and, compressive strength of geopolymers is directly correlated with alkali reactant ratio [30]. Si/Al and Na/Al molar ratios are other important parameters that affect properties of geopolymers; for instance, strength of geopolymers is influenced by initial silica content and setting of geopolymers is controlled by alumina content [30]. The role of water is critical in geopolymer systems because it is related with the workability of the mixture, dissolution of aluminosilicates, ion transfers and polycondensation of species [64, 65]; however, the content of it directly affects the alkalinity of medium, both high and low water content cause decrease in reaction rate [66]. Besides, water can be found in the final geopolymer product as free or bound water and microstructure of the geopolymer is influenced by free or bound water [65]. The last factor affecting properties of geopolymers is curing conditions. Curing conditions (curing time and temperature) has great influence on both mechanical properties and microstructure of geopolymers [67]. Strength of geopolymers has tendency to rise with increasing curing temperature and high curing temperatures provides gaining high early strength; nevertheless, if exposure time to high temperature is long, the strength of geopolymers may deteriorate in short and long term. Beside to possibility of loss of strength, cracking might be observed in geopolymers due to rapid loss of water at high curing temperatures [68].

In this study, structure-property relations of volcanic ash and perlite-metakaolin based geopolymers are investigated. In Chapter 2, the objective is to evaluate the potential utilization of volcanic ash in *one-part* geopolymer synthesis. Synthesized volcanic ash based *one-part* geopolymers with varying amounts of Si/Al and Na/Al molar ratios are characterized to determine structure-performance relationships in this system. In Chapter 3, perlite-metakaolin based foamed geopolymers with varying amounts of Si/Al and constant Na/Al molar ratios are synthesized with conventional methods.

X-ray diffraction (XRD), Fourier Transform Infrared (FTIR) Spectroscopy and Scanning Electron Microscopy (SEM) are applied for the characterization of both volcanic ash and perlite-metakaolin based geopolymers. Besides, compressive strength tests for volcanic ash based geopolymers; and Brunauer-Emmett-Teller (BET), Thermogravimetric Analysis (TGA), Differential Scanning Calorimetry (DSC) analysis and density measurements for perlite-metakaolin based geopolymers are performed. XRD analysis provides information about amorphous and crystalline phases in the product. Vibrational spectra of the geopolymers are determined by FTIR analysis. The microstructure of the samples is realized by means of the SEM analysis. Microstructure and mechanical performance of volcanic ash based geopolymers are correlated with compressive strength analysis. Microstructure, total pore volume and density of geopolymers are used to comprehend structure-property relationship in foamed specimens. Besides, thermal characteristics of geopolymers are determined by means of TGA and DSC analysis.

2. STRUCTURE – PERFORMANCE RELATIONS IN VOLCANIC ASH BASED ONE PART GEOPOLYMERS

2.1. Introduction

Geopolymers are amorphous aluminosilicates which are produced in alkaline environment and hardened at ambient or slightly elevated temperatures. There are three main reaction steps in geopolymerization: hydrolysis, oligomerization and polycondensation. When the alkali activator attacks to the surface of aluminosilicate raw material, hydrolysis reactions start and the reactive aluminosilicates in raw material dissolve and become free SiO_4 and AlO_4 tetrahedral units; then this step is followed by the formation of oligomers. Finally, these oligomers form 3-D aluminosilicate network by means of polycondensation reactions [47, 69, 70]. The structural and mechanical properties of the final product are affected by chemistry and mineralogy of the raw material, type and concentration of the alkali activator and curing conditions [46, 37, 45]. The type and concentration of the alkali activator, more specifically the available alkalinity in the environment, are critical for reactions because both the dissolution of aluminosilicates and polycondensation of oligomers are controlled by the activator [45, 71]. The traditional geopolymers synthesized by dissolving alkali activator in water before mixing with solid aluminosilicate precursor are referred as two-part geopolymers. This synthesis procedure has some disadvantages such as handling of corrosive and viscous alkaline solutions in commercial scale and scaling up problems [42]. Therefore, researchers started to focus on alternative geopolymers referred as *one-part* geopolymers that would be more convenient for commercial usage. These geopolymers are synthesized based on "just add water" concept which is similar to the utilization of conventional Portland cement. In this method, water is added to a solid mixture of aluminosilicate raw materials, alkali silicates and/or alkali hydroxides [70]. The studies in this growing area report that mechanical strengths of *one-part* mix geopolymers are comparable to the two-part mix geopolymers [42]; however, Ke *et al.* [45] suggest that *one-part* geopolymer precursors should be researched in detail in terms of their minerology and reaction mechanisms.

The authors also emphasize that highly alkaline environment (pH ~ 11) is required for the dissolution of aluminosilicate raw material and this is easily achieved with alkaline solutions in two-part mix geopolymers; on the other hand, the environment reaches slowly to higher alkalinity in *one-part* mix. Therefore, the possible way to overcome this problem in *one-part* mix geopolymers is selecting an aluminosilicate raw material which has high amount of easily leachable alkali [45, 46].

Aluminosilicates form approximately %60 of the earth's crust implying that they are the most abundant compound in the earth crust [42]. Volcanic ash is one of these aluminosilicate materials and it is a potential candidate for geopolymerization reactions. Volcanic ash is advantageous in geopolymerization since it does not require any thermal activation as 1:1 clays do; hence, this property provides low energy consumption and economic gain [12] . Besides, since volcanic ashes are formed and deposited on the surface during volcanic activities, surface mining also provides economic gain when compared to the other types of mining [14]. Nevertheless, there are only few researches on geopolymerization of volcanic ashes in the literature and no research about volcanic ash based *one-part* geopolymers. Studies focusing on volcanic ash based geopolymers point out low reactivity of volcanic ash in geopolymerization [72]. In order to address this issue, various processes are proposed to enhance reactivity of volcanic ash including calcination [9], alkali fusion [73] and mechanical activation [74] processes. Calcination process is an energy-intensive procedure requiring temperatures between 700 and 900 ºC. Alkali fusion process includes calcination of volcanic ash in the presence of NaOH at a relatively lower temperature (500 ºC). This procedure is considered to be limited because of the requirement of additional aluminosilicate sources in order to consume excess sodium hydroxide present in the system. Mechanical activation of volcanic ash is reported to increase the amount of amorphous phase as well as the number of reactive centers in the raw material and thus seems to be more effective than calcination procedures. When evaluated together, all of these procedures require additional energy requirements and/or cause extra complexities in large-scale utilization of volcanic ash in geopolymerization technology.

In this context, the focus of this study is i) to employ volcanic ash in as-received form without any pre-treatment procedure in synthesizing *one-part* geopolymers that are more convenient for industrial applications, and ii) to investigate the relations between structural characteristics and mechanical properties of these geopolymers. A set of geopolymers is prepared with varying amounts of Si/Al and Na/Al ratios in the regions of 2.5-4.5 and 1.1-5.1, respectively. These specimens are characterized by X-ray diffraction (XRD), Fourier Transform Infrared (FTIR) Spectroscopy and Scanning Electron Microscopy (SEM) - Energy Dispersive X-Ray Analysis (EDS) and compressive strength measurements in order to determine structure-performance relationships in this system.

2.2. Experimental

Volcanic ash used in this study is supplied by MK İnşaat from Manisa, Turkey. Chemical composition of volcanic ash is given in Table 2.1. Volcanic ash is milled and sieved to 100 μm to provide sufficient surface area for geopolymerization reactions. Table 2.2 summarizes the synthesis parameters employed for obtaining volcanic ash based *one-part* geopolymers. Volcanic ash particles are mixed with anhydrous sodium metasilicate particles for about 3 minutes to assure good blending of these solids and to attain a set of specimens with molar Si/Al ratios of 2.5, 3.0, 3.5:1, 4.0 and 4.5. Then, these solid mixtures are directly mixed with water using a water/solid (wt./wt.) ratio of 0.3. The mixtures are stirred for about 20 minutes at 400 rpm in a low shear stirrer (Heidolph, RZR 2041) and poured into 4cm X 4cm X 16cm steel molds. Geopolymer specimens are cured at 60°C for ten days under atmospheric conditions before structural characterization and performance measurements. The images of synthesized volcanic ash based geopolymers are illustrated in Figure 2.1.

Figure 2.1. Images of synthesized volcanic ash based geopolymers

Chemical structure and morphology of geopolymer pastes are analyzed by means of X-ray Diffractometer (XRD), Fourier Transform Infrared Spectrometer (FTIR) and Scanning Electron Microscopy (SEM) - Energy Dispersive X-Ray Analysis (EDS) and also compressive strengths of them are measured with servo-hydraulic test machine. The equipment and test conditions used in this study are defined below:

(i) Bruker D8 Discover X-Ray Diffraction system with a Cu $K\alpha_1$ radiation source operating with a voltage and current of 40 kV and 40 mA, and scanning with a step size of 0.01260° for 2θ from 10-90° was used for XRD measurements.
(ii) Perkin Elmer One Spectrometer was used for FTIR analysis to detect 650-2000 cm^{-1} spectral region.
(iii) FEI-Philips XL30 ESEM-FEG with SE/BSE detector and EDAX EDS Analysis System were used for morphology and elemental analysis.
(iv) Servo-hydraulic test machine (model: MTS) with capacity of 100 kN and loading rate 0.01 mm/s was used for compressive strength measurements of geopolymers.

Table 2.1. Chemical composition of (wt.%) volcanic ash

Chemical Composition	**Volcanic Ash (wt. %)**
SiO_2	45.7
Al_2O_3	18.3
Fe_2O_3	11.6
CaO	8.6
K_2O	5.2
Na_2O	3.9
MgO	2.6
TiO_2	2.3
LOI	1.9

Table 2.2. Mixture design parameters used in the synthesis of volcanic ash based *one-part* geopolymers. Geopolymers are named using their molar Si/Al and Na/Al ratios. For instance, VA2511 refers to volcanic ash based *one-part* geopolymer with molar Si/Al ratio of 2.5 and molar Na/Al ratio of 1.1.

Geopolymer ID	**Si/Al**	**Na/Al**	**Si/Na**	**Water/Solid (g/g)**
VA2511	2.5	1.1	2.2	0.3
VA3021	3.0	2.1	1.4	0.3
VA3531	3.5	3.1	1.1	0.3
VA4041	4.0	4.1	1.0	0.3
VA4551	4.5	5.1	0.9	0.3

2.3. Results and Discussions

The XRD pattern of volcanic ash used in this study is presented in Figure 2.2. It displays a broad diffraction peak (halo) between 2θ region of 15-35° demonstrating that volcanic ash predominantly consists of an amorphous structure. The crystalline phases detected in volcanic ash are augite ($(Ca,Na)(Mg,Fe,Al,Ti)(Si,Al)_2O_6$), albite calcian ($(Na,Ca)Al(Si,Al)_3O_8$), anorthite sodian ($(Ca,Na)(Si,Al)_4O_8$), diopside ($MgCaSi_2O_6$), hematite ($\alpha$-$Fe_2O_3$), maghemite ($\gamma$-$Fe_2O_3$) and nepheline ($(Na, K)AlSiO_4$). In Figure 2.3, FTIR spectra of volcanic ash is presented and it is seen that material has a broad absorbance peak at 974 cm^{-1} assigned to the internal vibrations of Si-O-T (T: Si, Al). Moreover, smaller broads peaks observed at 1374 cm^{-1}, 1637 cm^{-1} and 1740 cm^{-1} are assigned to bending (H-O-H) vibrations of bound water molecules [13, 10]. Surface morphology of volcanic ash obtained by SEM is given in Figure 2.4. SEM images illustrate that volcanic ash particles are small and aggregated.

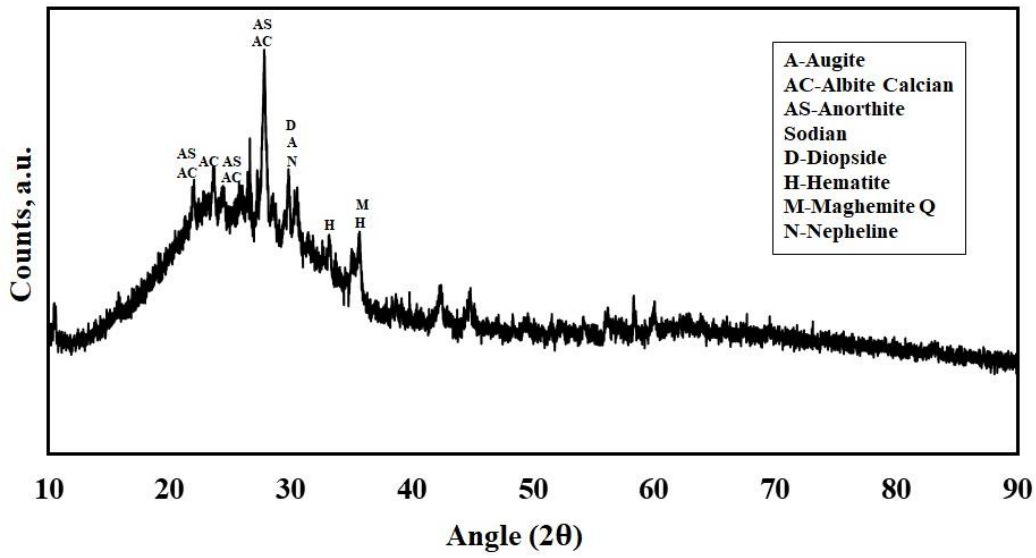

Figure 2.2. X-ray diffractogram of volcanic ash

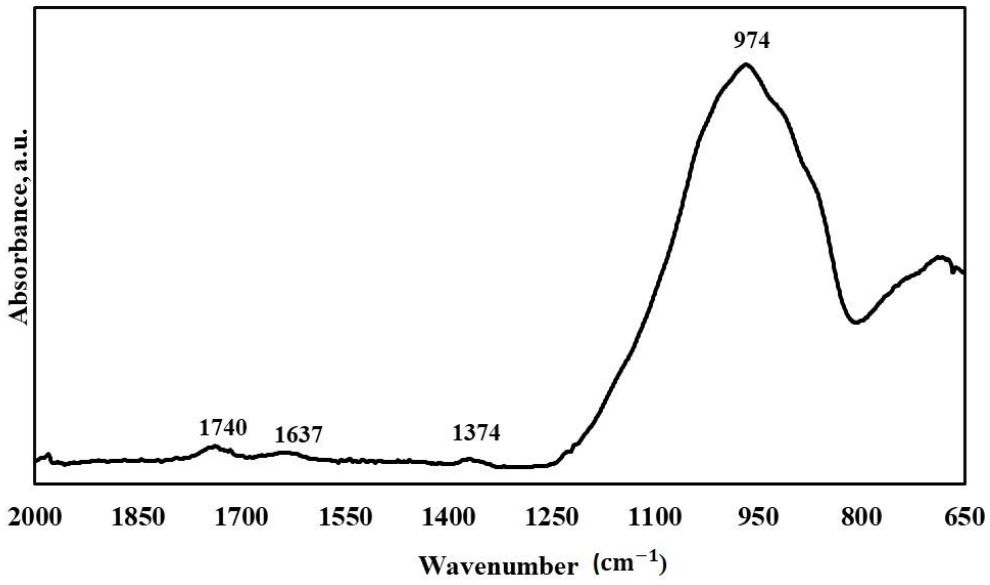

Figure 2.3. FTIR Spectra of volcanic ash

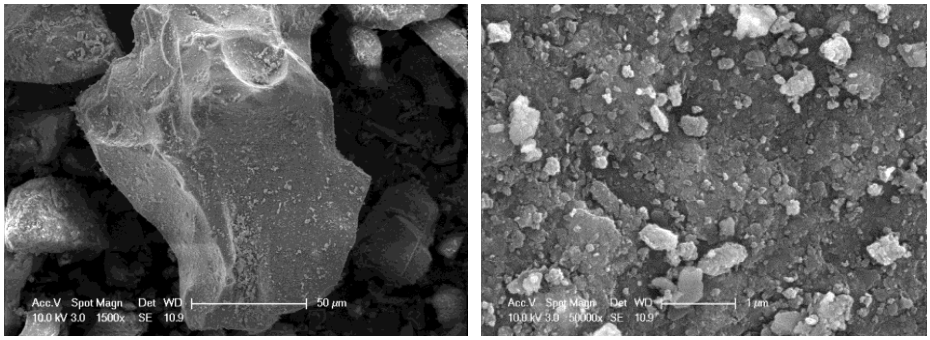

Figure 2.4. SEM images of volcanic ash

XRD patterns of volcanic ash based *one-part* geopolymers are given in Figure 2.5. A broad feature positioned between a 2θ region of 15-35° indicating amorphous aluminosilicate network [25, 32] exists together with crystalline phases found in the raw material for all of the specimens. Although conventional geopolymer structure is predominantly X-ray amorphous, the presence of crystalline phases in volcanic ash based geopolymers are mentioned in previous studies [13, 10, 12]. It is seen that the intensities of some of the crystalline diffraction peaks (albite, anorthite and nepheline) decrease as a function of increasing Si/Al and Na/Al ratios possibly due to the partial dissolution in alkaline environment and participation into the geopolymerization reactions. Specimen VA2511 seems to display higher degree of crystallinity compared to others. Increasing molar Si/Al and Na/Al ratios result in the appearance of an additional broad feature between 2θ of 10-15° in the XRD patterns of VA4041 and VA4551 possibly demonstrating the formation of a new amorphous phase in these specimens with higher molar Si/Al and Na/Al ratios. Besides to the dissolved crystalline phases, there are undissolved crystalline phases observed in all geopolymers. These are iron containing crystalline phases, hematite (α-Fe_2O_3) and maghemite (γ-Fe_2O_3). It is worthwhile to note the controversy about the role of iron in geopolymer systems in the literature. There are studies claiming that iron causes the removal of OH^- ions from the alkaline environment and this decelerates the dissolution of remaining aluminosilicates and prevents the formation of geopolymer network [12, 75, 76]. In the recent work of Kaya and Soyer-Uzun, it is reported that iron species in red mud tend to reprecipitate as goethite (FeO(OH)) removing OH^- ions from the alkaline environment affecting the geopolymerization and compressive strength development process in a negative fashion [76].

On the other hand, Perera *et al.* [77] and Lemougna *et al.* [78] reports that iron is not deleterious to the geopolymer formation; on the contrary, iron species take part in the formation of geopolymer structure either by integrating in the geopolymer network as isolated ions or as crystalline fillers in the form of oxyhydroxide aggregates. In the present study, reprecipitation of iron species in the form of hydroxides is not observed based on XRD results. It could be speculated that iron-containing crystalline phases tend to maintain their original form in the raw material and reside as microcrystalline phases serving possibly as fillers in glassy geopolymer matrices. As it is seen in Table 2.1, volcanic ash is somewhat rich in terms of calcium content. Previous studies [58, 33, 79] suggest high amount of CaO in the raw materials could lead to formation of amorphous calcium aluminosilicate gel during geopolymerization reactions causing reduction in microstructural porosity. This phenomenon contributes the improvement of mechanical properties of geopolymers [58, 80]. However, formation of a Ca–rich gel is not observed in this study based on XRD and SEM results.

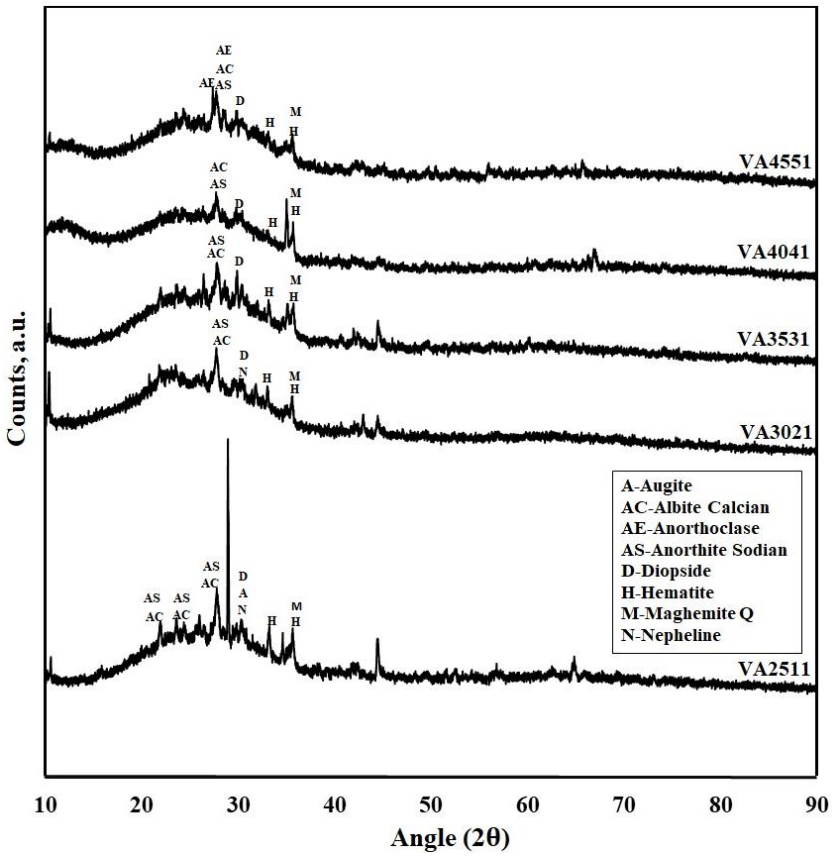

Figure 2.5. X-ray diffractograms of volcanic ash based *one–part* geopolymers

The FTIR spectra volcanic ash *one-part* geopolymers are given in Figure 2.6. FTIR spectra of the geopolymer specimens are characterized by the main absorption bands positioned between 900 cm^{-1} and 1000 cm^{-1} region. This main feature indicates asymmetric stretching vibrations of Si-O-T (T: Si, Al) in geopolymeric framework. The broad absorption band at 974 cm^{-1} for volcanic ash (Fig. 2.3) which is assigned to the asymmetric stretching vibrations of Si-O-T (T: Si, Al) bonds [81] clearly shifted to lower frequencies in geopolymers. This shift of the main band in volcanic ash (974 cm^{-1}) to lower frequencies as a result of alkali activation (967-922 cm^{-1}) is a significant indication of the geopolymerization reaction [82, 83]. It is also observed that FTIR main band systematically shifts to lower wavenumbers with concomitant increase in band intensity as Si/Al ratio increases in the system. A weak valley at 1657 cm^{-1} in the FTIR spectra of geopolymers VA4041 and VA4551 is attributed to the stretching (-OH) and bending (H-O-H) vibrations of water molecules [84]. The absorption bands located in the region of 1449-1467 cm^{-1} are assigned to the stretching vibrations of O-C-O bond which demonstrates the formation of sodium bicarbonate because of atmospheric carbonation [82]. This band loses its significance with increasing Si/Al (and Na/Al) ratio in the system. The features positioned at 885-887 cm^{-1} for specimens VA2511 and VA3021 are attributed to the bending vibration of Si-OH bonds in the geopolymer system [10]. It is seen that the dominance of Si-OH bands in geopolymers decrease with increasing molar Si/Al (and Na/Al) ratios (Figure 2.6).

Figure 2.7 presents the SEM morphologies of volcanic ash based *one-part* geopolymers at various length–scales. It is seen that the morphology of the volcanic ash (Figure 2.4) has changed into a glassy form upon geopolymerization. The surface morphologies of the specimens become denser and smoother at all length–scales as the molar Si/Al (and Na/Al) ratio increases in the system. Formation of glassy microstructure is an indication of geopolymerization reaction. Therefore, it is inferred that geopolymerization is achieved to a higher extend for the specimens with higher Si/Al (and Na/Al) ratios in volcanic ash based *one–part* geopolymers. Figure 2.8 presents SEM/EDS results of the geopolymers investigated in this study. These results confirm the formation of sodium aluminosilicate frameworks in the system as the major elements detected in the SEM/EDS spectra are Na, Al, Si and O. Additionally the presence of minor amounts of Fe is seen which might be related with the presence of hematite and maghemite phases.

It is hard to comment on the partial incorporation of Fe into the amorphous geopolymeric framework. Additional characterization techniques such as ^{57}Fe Mössbauer spectroscopy might be useful to comment on this issue [78].

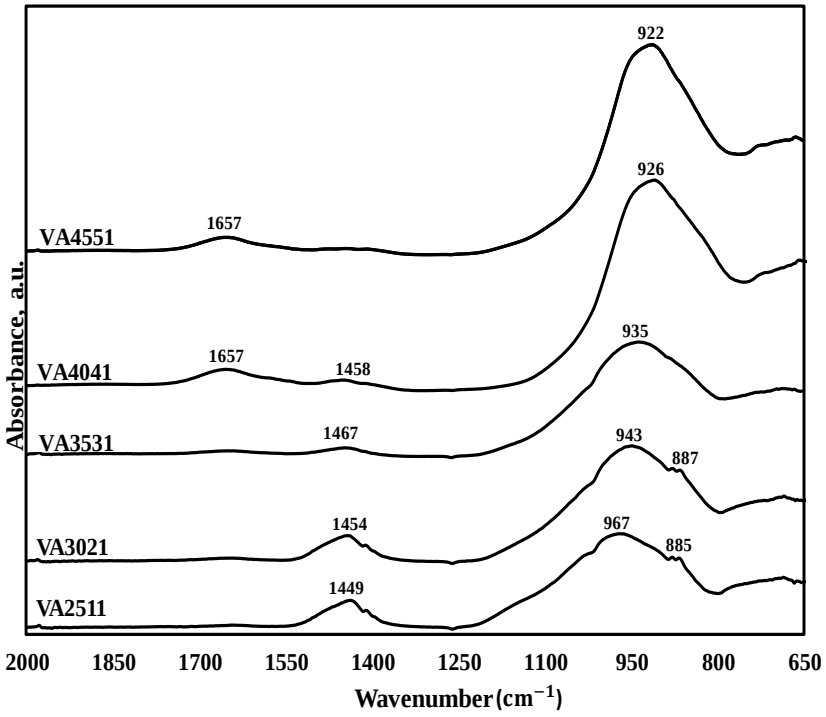

Figure 2.6. FTIR spectra of volcanic ash based *one–part* geopolymers

The compressive measurements are performed on the geopolymer specimens in order to complement the results obtained using structural characterization techniques. The compressive strength values of the geopolymer specimens are presented in Table 2.3. It is seen that these values monotonously increase with increasing molar Si/Al (and Na/Al) ratios.

Table 2.3. Compressive strength values of synthesized *one-part* geopolymers

Geopolymer ID	**Compressive Strength (MPa)**
VA2511	13.89
VA3021	14.28
VA3531	17.33
VA4041	12.70
VA4551	19.60

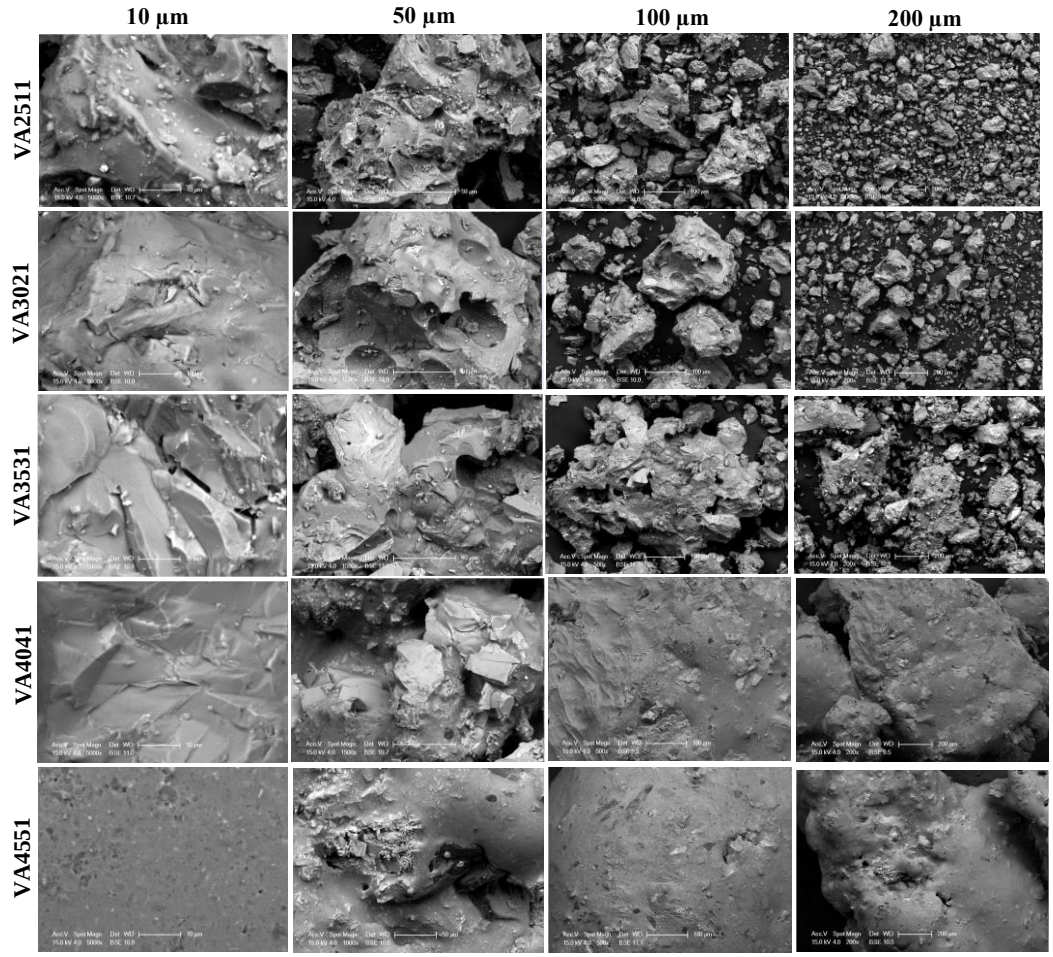

Figure 2.7. SEM microstructure of volcanic ash based *one-part* geopolymers

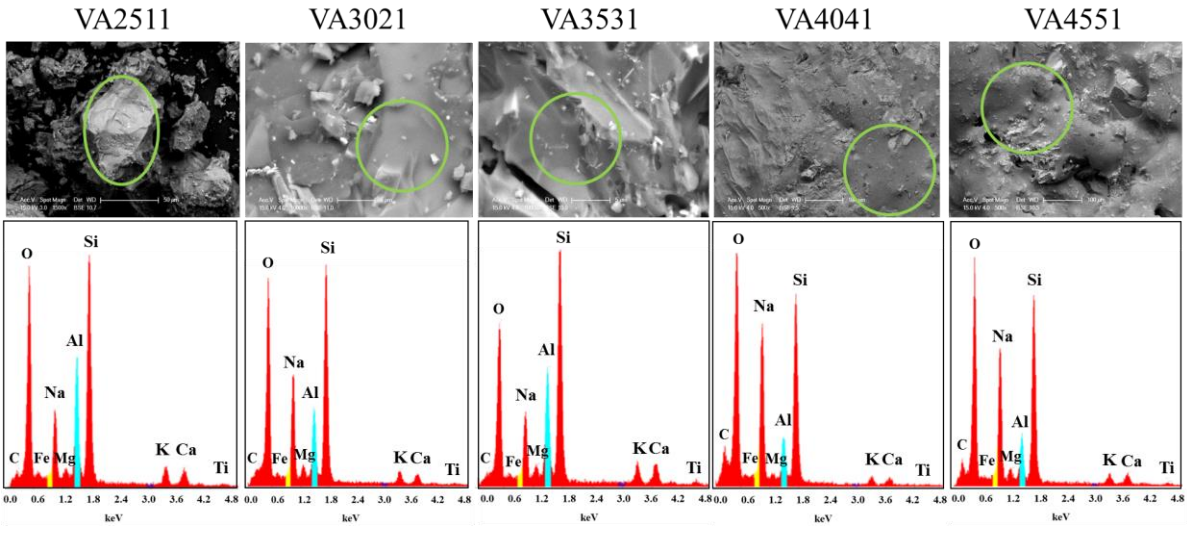

Figure 2.8. SEM/EDS spectra of volcanic ash based *one–part* geopolymers

Figure 2.9 illustrates the evolution of the main FTIR band position and compressive strength as a function of molar Si/Al (and Na/Al) ratio in the system. It is seen that compressive strength in the system constantly increases with increasing molar Si/Al ratios. Concomitantly, the main absorption band in the FTIR spectra constantly moves to lower values. Greater shift of this main band in the FTIR spectra of geopolymer specimens with respect to the main band in the FTIR spectrum of volcanic ash might indicate more changes in the chemical structure as a result of alkali activation. This finding is supported by the SEM microstructures that exhibited more binding effect at all length–scales with increasing Si/Al (and Na/Al) ratios (Figure 2.7). Therefore, evaluating FTIR spectroscopy, SEM images and compressive strength measurements together, it can be argued that geopolymerization is achieved to a higher extend for geopolymers with high molar Si/Al (and Na/Al) ratios. As pointed out previously, the absorption bands located in the region of 1449-1467cm^{-1} are related to the stretching vibrations of O-C-O bonds indicating the formation of sodium bicarbonate arising from atmospheric carbonation [82]. It is previously reported that geopolymerization reactions might be disrupted due to the presence of sodium carbonates [10]. Decrease in the intensity of this peak with the increasing Si/Al (and Na/Al) ratio of geopolymers seems to be correlated with the increasing compressive strength in the system. Additionally, the features positioned at 885-887 cm^{-1} indicating bending vibrations of Si-OH bonds [10] in the geopolymer system for specimens with lower molar Si/Al ratios (VA2511 and VA3021) disappear as molar Si/Al (and Na/Al) increases. It is previously pointed out that the presence of Si-OH in geopolymers leads to lower mechanical performance due to lower degree of polycondensation reaction [85]. This argument is confirmed by compressive strength measurements in this study.

It is important to note here that the optimum value of molar Si/Al and Na/Al ratios are reported to be around 2 and 1, respectively for attaining high compressive strength in traditional two-part metakaolin based geopolymer systems [25, 61, 86, 87, 88]. Besides, in volcanic ash based two-part geopolymer studies, Si/Al and Na/Al molar ratios changes between 2.6-2.9 and 1.0-1.75, respectively [13, 78]. On the other hand, the maximum compressive strength, among the geopolymers investigated in this work, is attained for the geopolymer specimen VA4551 with molar Si/Al and Na/Al ratios of 4.5 and 5.1, respectively.

It is known that mechanical properties of the geopolymers depend on a number of factors including the raw material, pre- and post- treatment procedures and conditions, and etc. However, this large difference in mixture compositions is thought to be mainly related to the nature of the raw material used in geopolymer synthesis. It is reported that the factors such as low dissolution of volcanic ash in alkaline solution, its mineral content and degree of crystallinity are related to its low reactivity compared to other aluminosilicate sources [72]. In this regard our results support previous findings highlighting the requirement of greater molar Si/Al ratios for better properties in volcanic ash based geopolymer systems [13]. Additionally, it is important to note that *one–part* geopolymer systems require a whole new concept of geopolymer design as the availability and the dissolution of aluminate and silicate species in *one–part* systems are different compared to traditional two part systems possibly leading to different reaction mechanisms [89]. Therefore, it would be beneficial if future research efforts are directed toward understanding geopolymerization kinetics and optimizing synthesis conditions for maximum performance in volcanic ash based geopolymer systems.

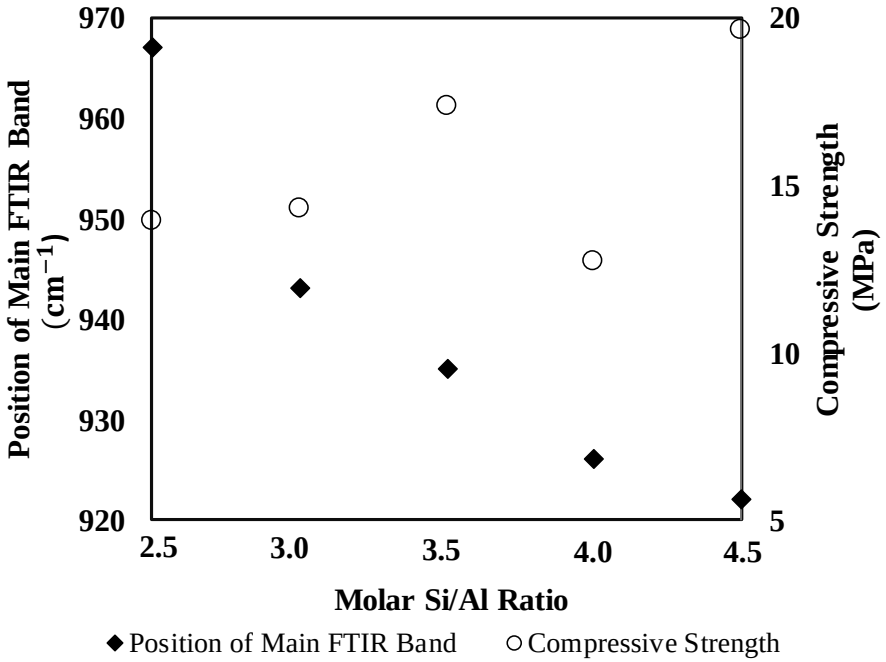

Figure 2.9. The position of main FTIR band in geopolymers in the FTIR spectra of geopolymers and compressive strength of geopolymers as a function of molar Si/Al ratios

2.4. Conclusion

Volcanic ash based *one–part* geopolymers with varying compositions such that molar Si/Al and Na/Al ratios are in the ranges of 2.5–4.5 and 1.1–5.1, respectively, are synthesized employing volcanic ash without any pre–treatment procedures. A variety of structural characterization methods including XRD, FTIR spectroscopy, SEM analysis and compressive strength measurements are performed in order to determine structure-performance relationships in this system. XRD results indicate that the crystalline phases (albite, anorthite and nepheline) in volcanic ash seem to dissolve and participate into the geopolymer network as Si/Al ratio increases in the system; nevertheless, iron based crystalline phases (hematite and maghemite) are detected together with some aluminosilicate minerals in the amorphous geopolymer matrix acting as microcrystalline fillers. The main absorption band in the FTIR spectrum of volcanic ash is located at 974 cm^{-1}. Upon alkali activation, the position of this main band shifts to 967 cm^{-1} for the specimen with molar Si/Al ratio of 2.5 (VA2511). Further increase in molar Si/Al (and Na/Al) ratio results in more pronounced and systematic shifts in the position of the main bands to much lower wave numbers. These changes are coupled with loss of intensities of FTIR bands corresponding to Si–OH and carbonates. These systematic changes are correlated with the increasing trend in the compressive strength values of these specimens. SEM/EDS analyses support these findings demonstrating that glassy morphologies of the geopolymer specimens notably become smoother as molar Si/Al (and Na/Al ratios) increases in the system. The structure-performance relationship is established by compressive strength measurements and the highest compressive strength value, 19.6 MPa, is achieved for Si/Al molar ratio of 4.5. To conclude, volcanic ash could be utilized as raw material in *one-part* geopolymer synthesis and the optimum Si/Al molar ratio for one part geopolymers is determined as 4.5 for this study.

3. STRUCTURAL, PHYSICAL AND THERMAL CHARACTERISTICS OF PERLITE-METAKAOLIN BASED FOAMED GEOPOLYMERS

3.1. Introduction

Amorphous aluminosilicates synthesized by the alkali activation of aluminosilicate materials is named as geopolymers that is first coined by Davidovits in the late 1970's. Geopolymers are alternative materials for ordinary Portland cement (OPC) because of the fact that their synthesis method is simple, energy efficient and eco-friendly when compared to the OPC [7]. During synthesis, a polymeric silicon-oxygen-aluminum framework structure is constituted by multistep simultaneous reactions of Al-Si materials in highly alkaline environment [30, 90]. The reaction mechanism can be explained in three steps:

(i) Dissolution of raw material in alkaline environment to leach Al and Si species
(ii) Polymerization of these soluble species to form oligomers
(iii) Finally, polycondensation of oligomers and formation of 3-D aluminosilicate structure

This mechanism does not depend on starting raw materials and any material containing Si and Al bearing phases could become source for synthesis of geopolymers [80, 91]. Geopolymers display a wide range of properties and these properties are directly affected by aluminosilicate raw material and alkaline activator [92], by altering these parameters, one can tailor properties of geopolymers for specific applications [93]. High mechanical strength, durability against aggressive conditions (high acidity, chemical exposure, fire etc.), lightweight and thermal stability are some of the excellent physical and mechanical properties of geopolymers [30]. As mentioned before, these diverse properties provide different application areas such as green cement & concrete, fire & heat resistant composites, radioactive & toxic waste encapsulation and thermal insulators.

Lightweight porous materials are used in construction industry to construct lighter buildings, to decrease steel and concrete consumptions, to improve thermal properties and fire resistance of buildings [94]. Autoclaved aerated concrete (AAC) dominates the market as lightweight porous materials. These lightweight porous materials are mostly produced by foaming of ordinary Portland cement through hydrogen gas; after that resulting product is subjected to 180-200°C and 8-12 bars steam pressure in autoclave to fulfill enough mechanical strength [94, 95, 96]. Although these materials have significant advantages, drawbacks of process such as being energy intensive and usage of explosive gas cannot be ignored [94]. Therefore, synthesis of foamed geopolymers would be a good alternative for AAC.

Formation of closed cells (small individual voids) or open cells (interconnected series of voids) inside the material take place during foaming process, and nature, size and distribution of these voids are crucial parameters for determination of density and strength of foamed materials. There are two methods to generate voids in sample [94]:

(i) Utilizing gas releasing agents (H_2O_2, fine aluminum or zinc powders) in the mixture to lead endogenous gas generation
(ii) Usage of organic foaming agent to attain large volume fraction of air bubbles

In this study, perlite and metakaolin are selected as aluminosilicate raw material for the synthesis of foamed geopolymers. Perlite is exploited by surface mining which provides economic gain in comparison to other types of mining and Turkey has more than half of the known perlite reserves (~7 billion tones) in the world [15, 20, 21, 22]. Metakaolin is also utilized in this study to take the advantage of its high reactivity and relatively pure elemental composition with respect to the other aluminosilicate raw materials. The main objective of this study is to analyze the structural, physical and thermal properties of foamed geopolymers synthesized employing perlite and metakaolin as aluminosilicate raw material, which are foamed by using hydrogen peroxide as blowing agent.

The synthesized geopolymers are characterized by means of X-ray diffraction (XRD), Fourier Transform Infrared (FTIR) Spectroscopy, Scanning Electron Microscopy (SEM), Thermogravimetric analysis (TGA), Differential Scanning Calorimetry (DSC) and Brunauer-Emmett-Teller (BET) analysis together with the density measurements.

3.2. Experimental

Metakaolin is obtained by calcination of kaolinite at 750 °C for 3 hours and this process provides removal of water molecules between Al and Si layers in kaolinite and activates metakaolin for geopolymerization process. Perlite is used in its received form. The particle size of the specimen is between 74-300 μ. Chemical compositions of perlite and metakaolin are received by XRF spectroscopy and are given in Table 3.1. As Table 3.1 illustrates metakaolin is relatively pure compared to the perlite.

6M sodium hydroxide (NaOH) solution is used as alkaline activator and hydrogen peroxide (H_2O_2) solution %50 w/w is used as chemical blowing agent that leads to foaming of pastes. Oxygen gas released by decomposition of hydrogen peroxide provides blowing of geopolymeric pastes.

Table 3.1. Chemical compositions (wt%) of perlite and metakaolin

Chemical Composition	**Perlite (wt%)**	**Metakaolin (wt%)**
SiO_2	73.7	56.2
Al_2O_3	14.5	41.0
Fe_2O_3	1.30	0.36
CaO	1.13	0.09
K_2O	5.97	0.46
MgO	0.64	0.07
TiO_2	0.17	1.15
Na_2O	1.83	-

Perlite and metakaolin are thoroughly mixed (for 10 minutes) with metakaolin percentages 0, 10, 20, 30, 40, 50 and 100 (wt %). After dry mixtures are prepared, 6 M NaOH solution is added to mixture and resulting paste is mixed for 10 minutes. After that 3% (wt/wt) H_2O_2 is mixed with the pastes and final geopolymer products are cured at room temperature. These dry mixtures are named as GP100P, GP90P10M, GP80P20M, GP70P30M, GP60P40M, GP50P50M and GP100M; and molar Si/Al and Na/Al ratio of these mixtures are tabulated in Table 3.2. The images of synthesized foamed geopolymers are illustrated in Figure 3.1.

Table 3.2. Molar ratios used in perlite-metakaolin based geopolymers
(P: Perlite, M: Metakaolin)

Geopolymer ID	Si/Al	Na/Al	Water/Solid (g/g)	Thermal Treatment
GP100P	4.3	1.0	0.23	8 weeks at 25 °C
GP90P10M	3.3	1.0	0.33	8 weeks at 25 °C
GP80P20M	2.7	1.0	0.42	8 weeks at 25 °C
GP70P30M	2.3	1.0	0.51	8 weeks at 25 °C
GP60P40M	2.0	1.0	0.59	8 weeks at 25 °C
GP50P50M	1.8	1.0	0.67	8 weeks at 25 °C
GP100M	1.2	1.0	1.02	8 weeks at 25 °C

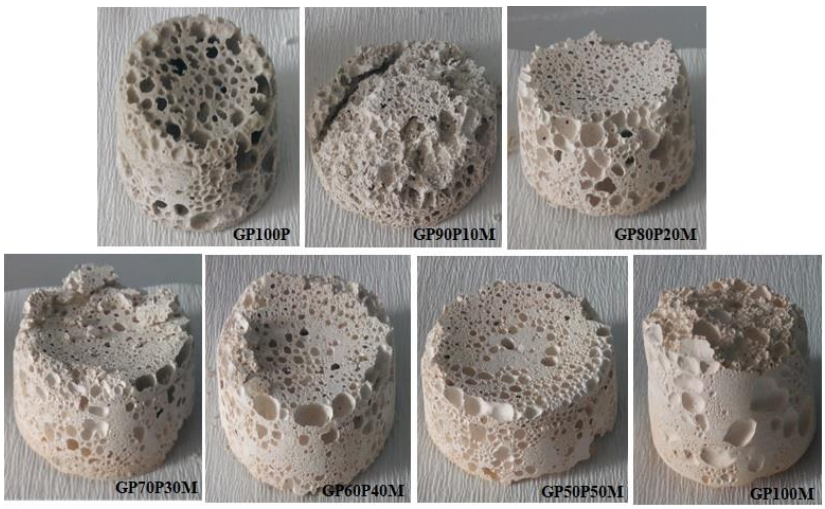

Figure 3.1. Images of synthesized perlite-metakaolin based foamed geopolymers

X-ray Diffractometer (XRD), Fourier Transform Infrared Spectrometer (FTIR) and Scanning Electron Microscopy (SEM) are used for studying chemical structure and morphology of geopolymers. Thermogravimetric analysis (TGA) and Differential Scanning Calorimetry (DSC) analysis are conducted to understand thermal behavior of geopolymers at elevated temperatures. Brunauer-Emmett-Teller (BET) analysis is performed to predict total surface area of samples; and Barrett-Joyner-Halenda (BJH) method is used to obtain pore volume and pore diameter of samples. Besides, densities of samples are measured by water pycnometer method at 25°C as illustrated in Figure 3.2:

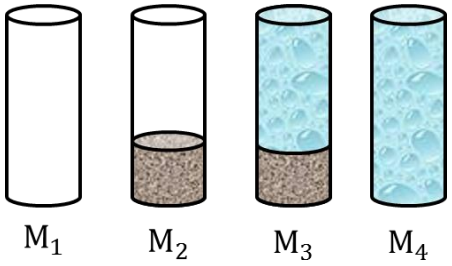

Figure 3.2. Schematic illustration for the determination of densities of geopolymers by water pycnometer

M_1: mass of empty pycnometer

M_2: mass of the pycnometer with dry sample

M_3: mass of the pycnometer and sample and water

M_4: mass of pycnometer filled with water

$$\text{Density of sample} = \frac{M_2 - M_1}{(M_2 - M_1) - (M_3 - M_4)} \quad (3.1)$$

The equipment and test conditions used in this study are defined below:

(i) Bruker D8 Discover X-Ray Diffraction system with a Cu $K\alpha_1$ radiation source operating with a voltage and current of 40 kV and 40 mA, and scanning with a step size of 0.01260° for 2θ from 10-90° was used for XRD measurements.

(ii) Perkin Elmer One Spectrometer was used for FTIR analysis to detect 650-2000 cm^{-1} spectral region.

(iii) Zeiss Ultra Plus (FEG-SEM) with a secondary electron (SE) detector was used for morphology analysis.

(iv) Perkin Elmer TGA 4000 and DSC 4000 instruments were used to evaluate the thermal properties of samples in the range of 35-1000 °C and -60-200 °C, respectively. Analyses were performed with 5-10 mg sample in a nitrogen flow at heating rate of 5 °C/min.

(v) BET surface area measurements were performed on a Micrometrics ASAP 2020– Physisorption Analyzer. Approximately 300 mg of samples were degassed at 200 °C for 8 h then N_2 adsorption was applied samples determine surface areas and pore diameter properties.

3.3. Results and Discussions

Metakaolin is obtained by calcination of kaolinite at 750 °C and during this process the crystalline structure of the kaolinite turns into amorphous structure [25] as illustrated in Figure 3.3. XRD patterns of both metakaolin and perlite have a broad halo peak between *2θ* region of 15-30° which is centered at 23°. This feature indicates that perlite and metakaolin consist of amorphous structures. Crystalline phases are also observed in addition to these amorphous structures. Metakaolin involves quartz (SiO_2); perlite includes albite ($NaAlSi_3O_8$) and anorthite ($CaAl_2Si_2O_8$) crystalline phases as it is seen in XRD patterns (Figure 3.3). In Figure 3.4, the FTIR spectra of metakaolin and perlite are presented. Broad absorbance peak at 1080 cm^{-1} corresponds to stretching vibration of Si-O-T (T: Si, Al) in metakaolin network [97]. Besides, the band at 815 cm^{-1} in metakaolin samples are attributed to vibrations of AlO_4 [76]. Perlite also have intense and broad feature at 1035 cm^{-1} that is assigned to Si-O-Si and Si-O-T (T: Si, Al) asymmetric stretching vibrations [98]. The medium intensity peak at 792 cm^{-1} is attributed to symmetrical stretching of Si-O-Si bonds [15, 98, 99].

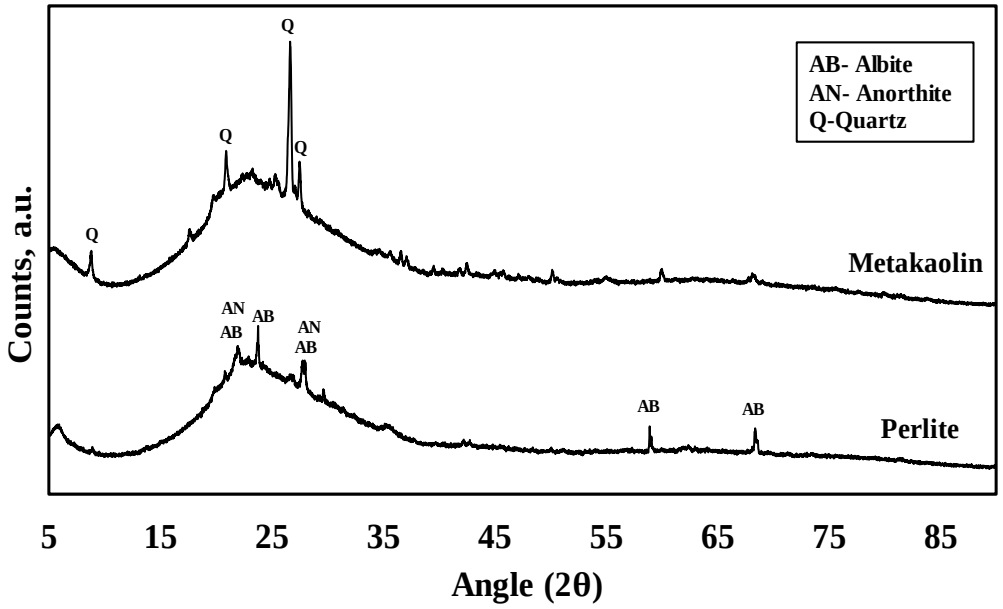

Figure 3.3. XRD diffractograms of perlite and metakaolin

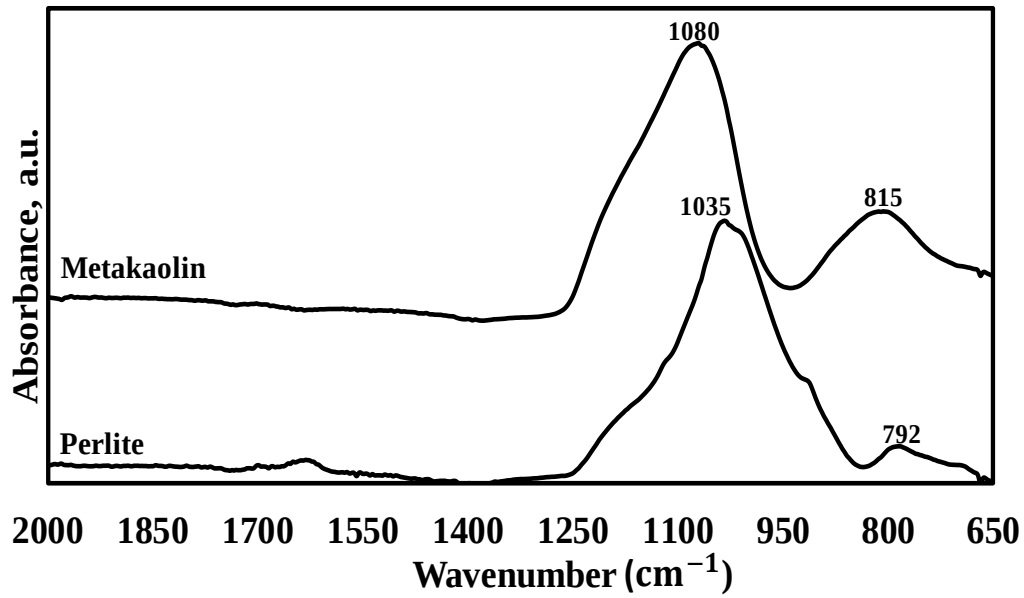

Figure 3.4. FTIR spectra of perlite and metakaolin

Figure 3.5 displays SEM morphologies of perlite and metakaolin. Metakaolin particles are platy in shape, less bulky and less hexagonally shaped when compared to kaolinite particles due to the calcination [100].

Perlite particles, on the other hand, display rough and much denser microstructures. BET surface area values also verify that microstructures of these two raw materials differ from each other. The surface areas of perlite and metakaolin are measured as 2.48 and 13.94 m^2/g, respectively. Besides, density values of perlite and metakaolin are 2.16 and 2.39 g/cm^3, respectively.

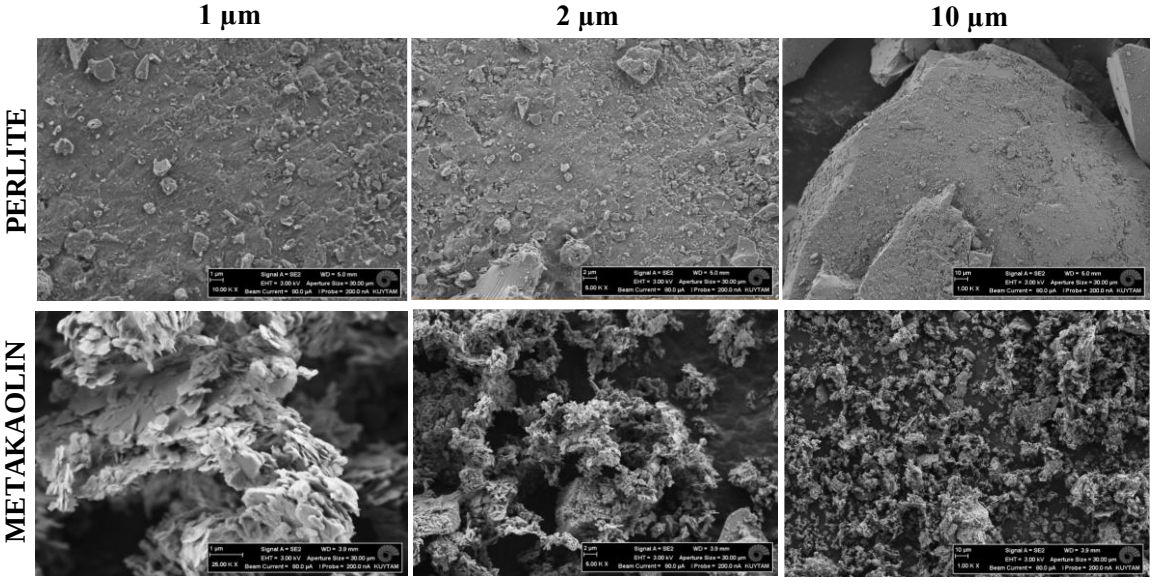

Figure 3.5. SEM images of perlite and metakaolin

Figure 3.6 and 3.7 represent termogravimetry curves (TG) and differential scanning calorimetry (DSC) analysis thermograms of perlite and metakaolin, respectively. It is seen in Figure 3.6 that weight loss of perlite is greater than that of metakaolin; namely, the weight losses of perlite and metakaolin are 4.59% and 2.82%, respectively. In literature, it is stated that perlite has 2-5 % (wt.) combined water [16, 17, 18] and according to the Figure 3.6, the water contained in matrices is gradually lost as the material is heated in the region of 400-1000 °C. The weight loss of perlite (4.59%) is also coherent with the range specified as combined water in the literature. As it is seen in Figure 3.7, there are no specific peaks in DSC thermograms of perlite and metakaolin in the temperature range of between -60 and 200 °C.

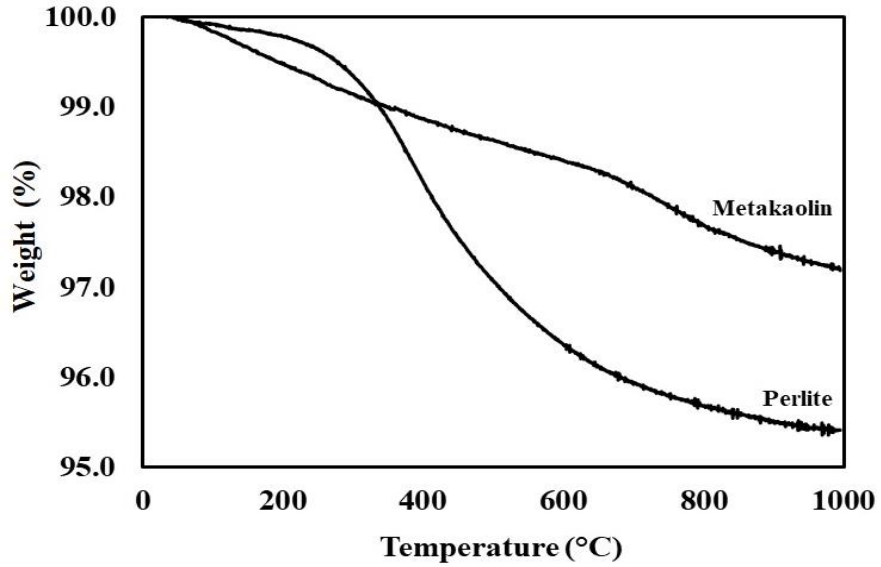

Figure 3.6. Thermal Gravimetric Analysis (TGA) of perlite and metakaolin

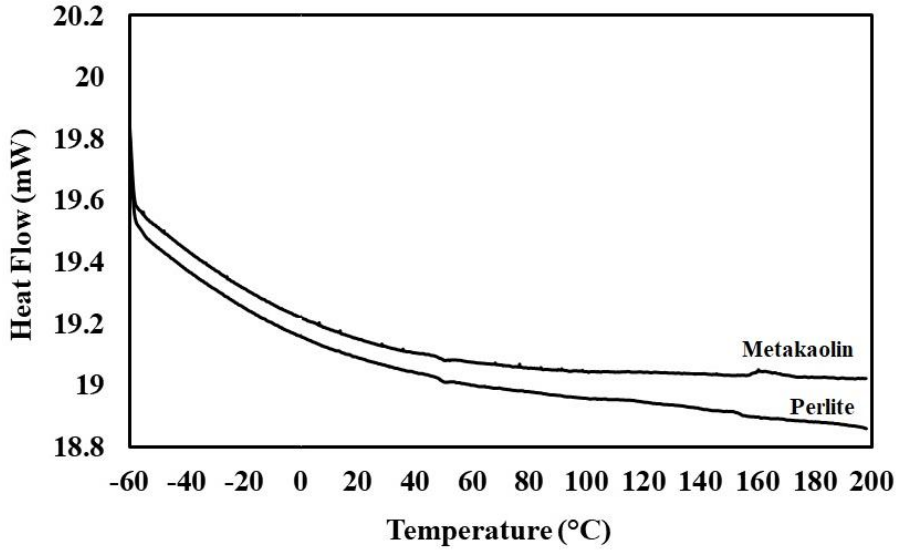

Figure 3.7. Differential Scanning Calorimetry (DSC) analysis of perlite and metakaolin

Figure 3.8 displays XRD patterns of geopolymers studied in this chapter. Geopolymer specimen GP100P displays an amorphous structure and the halo peak centered at 23° in its XRD pattern is similar to that of perlite. The center of gravity of this feature constantly shifts to higher angles as metakaolin content in the system increases.

However, the crystalline diffraction peaks (albite and anorthite) observed in perlite are not seen any more in GP100P, which indicates that these phases are dissolved in alkaline solution and participated into the geopolymerization reactions. The diffraction pattern of GP100P shows new crystalline peaks which are quartz (SiO_2), anorthoclase ($(Na,K)AlSi_3O_8$), sodium aluminosilicate ($AlNaO_6Si_2$) and termonatrite ($Na_2CO_3.H_2O$). GP90P10M geopolymer displays a somewhat similar diffraction pattern to that of perlite because of the fact that albite crystalline phases are observed clearly in geopolymer also. It has been reported that increase of the SiO_2/Na_2O ratio in the system, when Na/Al ratio is kept constant, results in formation of larger oligomers in solution and these oligomers could not undergo geopolymerization reaction due to the fact that they are not able to dissolve and react quickly [101, 102] . Uncondensed species that are more reactive than others control the reactivity of solution [103, 104]. Therefore, it can be claimed formation of large oligomers in GP100P and GP90P10M geopolymers might have disrupted geopolymerization reactions. As metakaolin percentage increases in geopolymers (GP80P20M, GP70P30M, GP60P40M, GP50P50M and GP100M); in other words, as Si/Al molar ratio reduces from 2.7 to 1.2, the formation of zeolite A and sharp quartz peak stand out in XRD diffractograms. The quartz peak must be originating from metakaolin sample as quartz phase is present in the XRD pattern of metakaolin. Zeolite A formation is not seen in GP100P and GP90P10M geopolymers which have molar Si/Al ratios of 4.3 and 3.3, respectively and this result is consistent with the literature due to the fact that Provis *et al.* [105] states that as silica concentration in the solution increases, the formation of zeolites are suppressed. In addition to zeolite and quartz crystalline phases, major phases displayed in GP80P20M geopolymer are anorthite ($CaAl_2Si_2O_8$), moganite (SiO_2) and albite ($NaAlSi_3O_8$). Formation of potassium aluminum silicate ($KAl_4Si_2O_{12}$) crystalline phase is identified for geopolymers GP60P40M and GP50P50M. GP100M geopolymer, moreover, displays microcline ($KAlSi_3O_8$) crystalline phase that is not observed for other geopolymers. Besides to crystalline phases observed, it is clearly seen in XRD patterns that as Si/Al molar ratio decreases, the amorphous halo peak shifts to higher angles (~27-29° 2θ) and Davidovits points out that structure becomes more polymerized with shifting to higher angles [106].

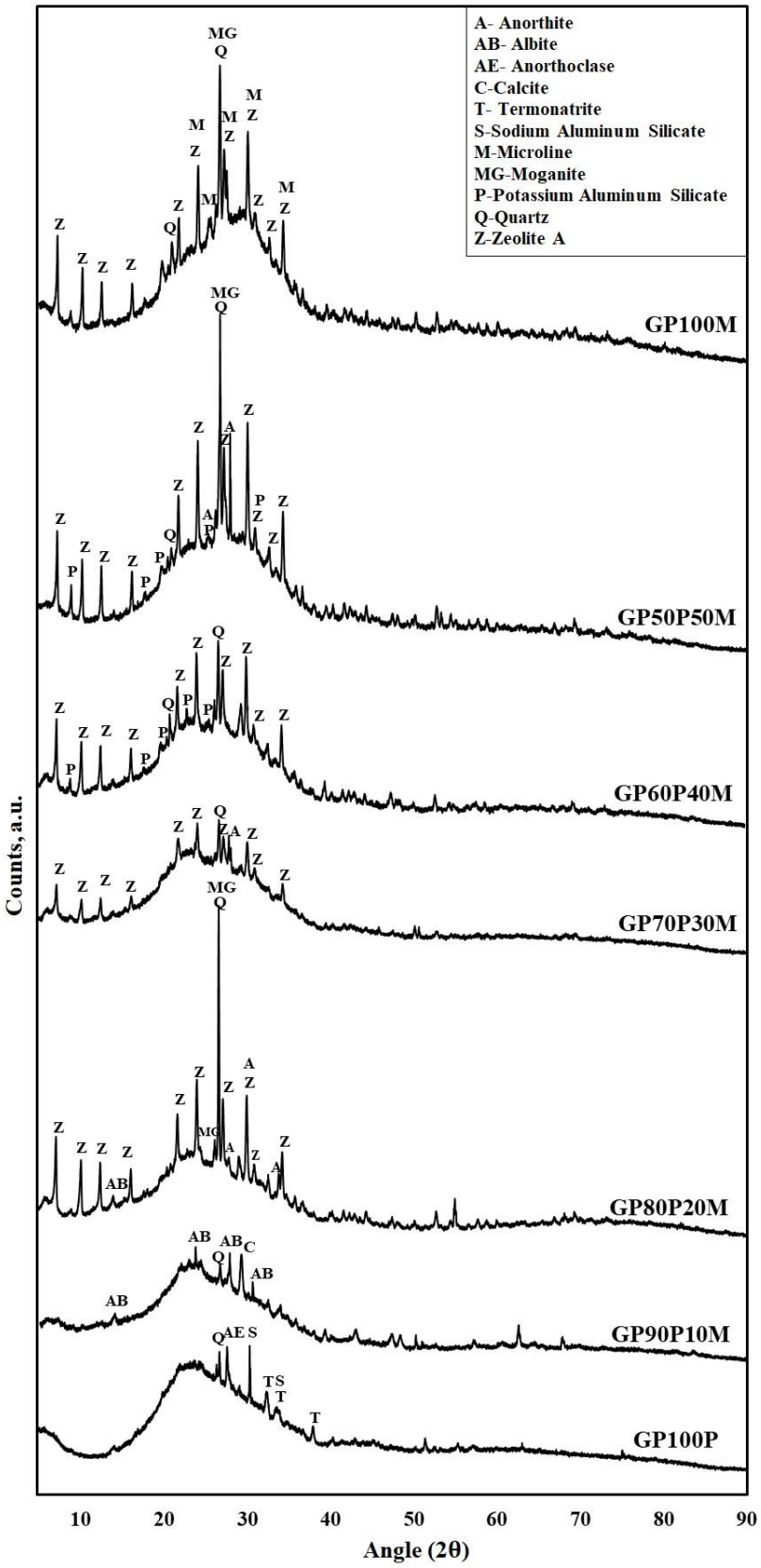

Figure 3.8. XRD diffractograms of perlite-metakaolin based geopolymers

Figure 3.9 displays FTIR spectra of geopolymers. A wide and intense band, named also as "main band", is observed in the region of 900-1200 cm^{-1} in all FTIR spectra of geopolymers. The bands around 1000 cm^{-1} are attributed to the quartz, amorphous silica and Si-O symmetrical vibrations, and the bands around 1100 cm^{-1} are attributed to asymmetric stretching band of pure SiO_2. As aluminum participates into the network, the intensity of these bands shifts to lower wavenumbers [15, 107, 108]. Davidovits [109] reports that the level of geopolymerization is related with the amount of shift in this main band. The main bands are positioned at 1080 cm^{-1} and 1035 cm^{-1} for metakaolin and perlite, respectively as shown in Figure 3.4. This main band shifts to lower frequencies (990-957 cm^{-1}) in geopolymers as Si/Al molar ratio decreases. Shifting of this strong band is related with the formation of sodium aluminosilicates as result of geopolymerization reactions. During reactions, SiO_4 species are partially replaced with AlO_4 species and this replacement leads to alteration in the local environment of Si-O bonds [15, 25]. The bands at ~850 cm^{-1} which is assigned to AlO_4 stretching vibrations is also observed for all geopolymers but the intensity of this peak reduces as Si/Al molar ratio decreases. The absorption band located at 1464 cm^{-1} for GP100P and GP90P10M geopolymers is attributed to the stretching vibrations of O-C-O bond indicating that carbonate species exist in the samples [82] and presence of sodium carbonates might disrupt the geopolymerization reactions [10]. When GP100P and GP90P10M geopolymers are compared with other geopolymers, their main absorption peak is not sharp or intense as others; this might be due to the presence of carbonate species. The weak bands at ~1657 cm^{-1} for all geopolymers is assigned to the bending (H-O-H) vibrations of water molecules because of the adsorbed atmospheric water [84].

SEM morphologies of geopolymers are presented in Figure 3.10. GP100P geopolymer exhibits denser and rougher matrix when compared to the other geopolymer specimens. As metakaolin percentage increases in geopolymer samples, the microstructure of geopolymers alters dramatically and dense structure is no longer observable. For instance, the formation of crystalline zeolite A cubes in GP80P20M geopolymer draws attention, which is consistent with XRD diffractograms.

Another distinctive observation in SEM images is randomly grown needles in clusters on the surfaces of gels that contain at least 30 % (wt/wt) metakaolin. These structures could be attributed to Na-rich crystals [110]. Unreacted metakaolin particles that are platy in shape are seen in SEM micrographs of GP50P50M and GP100M geopolymers.

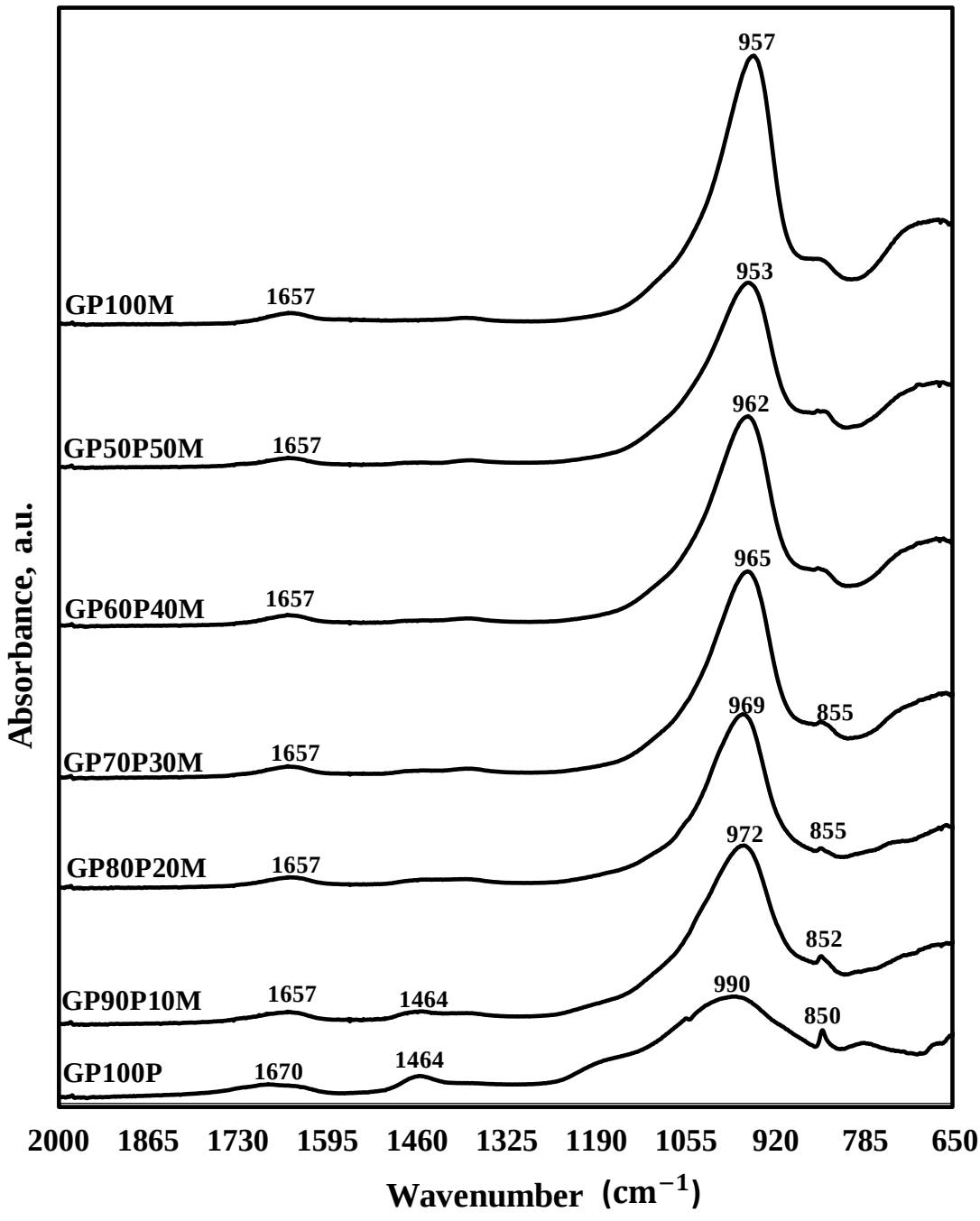

Figure 3.9. FTIR spectra of perlite-metakaolin based geopolymers

Besides to morphology, in Figure 3.1, it is clearly seen that all geopolymer specimens have pores on their surfaces due to decomposition of H_2O_2. N_2 gas sorption analyses and density measurements are conducted to gather more data about distribution of the pore sizes of the geopolymer samples and their physical properties. The results of N_2 gas sorption analyses and density measurements are tabulated in Table 3.3.

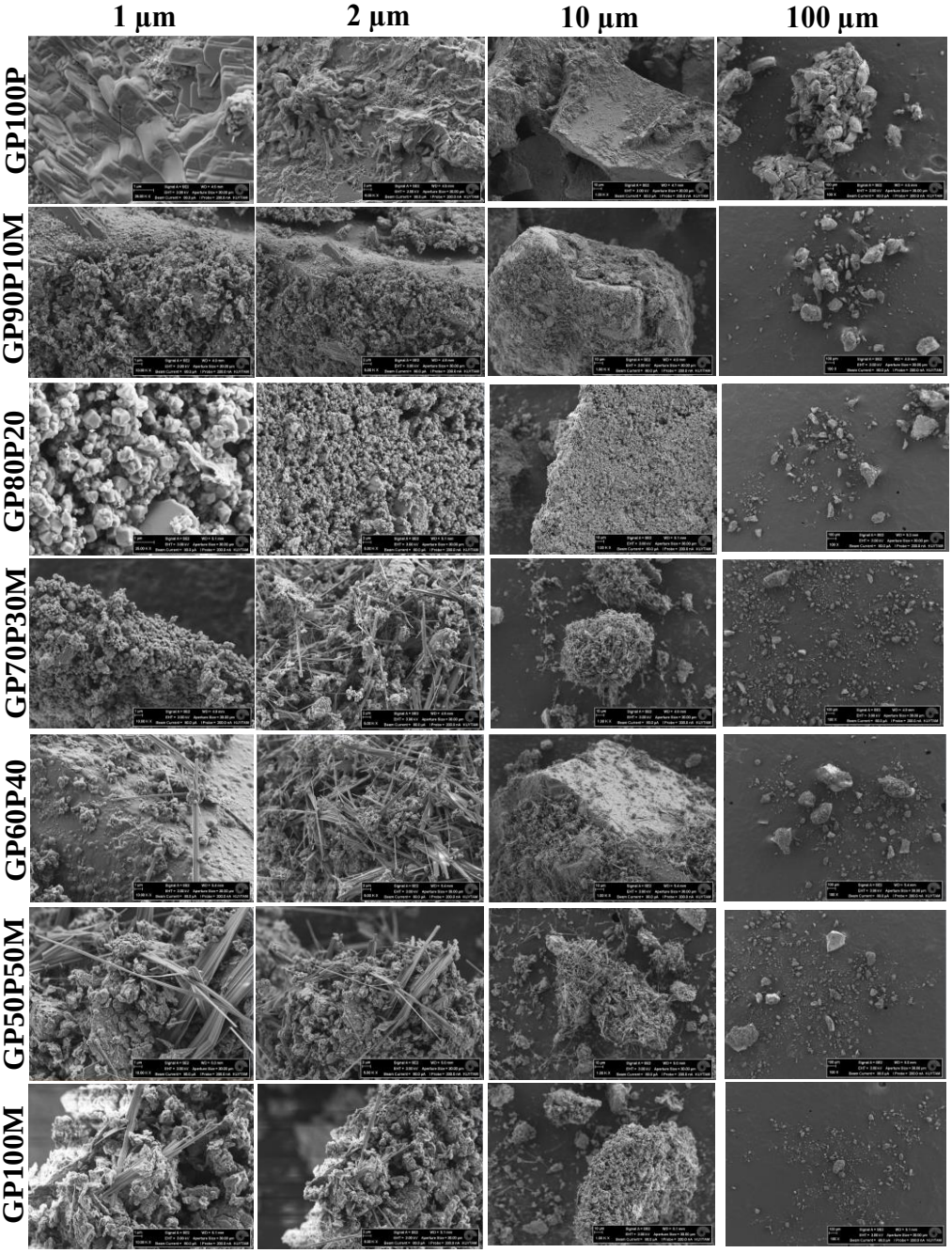

Figure 3.10. SEM images of perlite-metakaolin based geopolymers

Table 3.3. Results of N_2 gas sorption analyses and density measurements

Geopolymer ID	**Density (g/cm^3)**	**BET Surface Area (m^2/g)**	**Total Pore Volume (cm^3/g)**	**Average pore diameter (nm)**
GP100P	2.343	0.22	0.0055	122.9
GP90P10M	2.305	1.59	0.0047	60.56
GP80P20M	2.201	16.5	0.0057	44.32
GP70P30M	2.127	7.85	0.0051	42.45
GP60P40M	2.055	7.81	0.0061	45.79
GP50P50M	1.965	6.05	0.0065	49.79
GP100M	1.739	5.29	0.0138	30.62

Perlite-metakaolin based geopolymers are foamed with 3% (wt/wt) hydrogen peroxide to provide volume expansion and porosity in samples. Expansion or densification of geopolymers are greatly influenced by chemo-physical equilibrium between aluminosilicate raw material, formation of gel and pore coalescence; accordingly, density and expansion behavior of geopolymers could variate sample to sample [111]. Figure 3.1 clearly indicates that all geopolymer samples have irregularly shaped macropores as a result of foaming process. The morphology and distribution of pores depends on several factors such as reactivity of aluminosilicate raw material, viscosity and homogeneity of solution [104, 112].

Table 3.3 represents the parameters that are determined by N_2 gas sorption and water pycnometer for each geopolymer sample. BET surface area and total pore volume values range between 0.22-16.5 m^2/g and 0.0047-0.0138 cm^3/g, respectively. Zhang *et al.* [113] points out that water/solid ratio and SiO_2/Na_2O mass ratio affect the porosity of geopolymers; in other words, if water/solid ratio value gets larger or SiO_2/Na_2O mass ratio gets smaller, porosity of geopolymers increases. In this study, GP100P geopolymer has the lowest total pore volume, hence it is expected that this specimen should have highest density and density is measured as 2.343 g/cm^3.

This result is in compliance with the literature and SEM images (Figure 3.10), and one can see that the most rough and dense image among the geopolymers is acquired for GP100P geopolymer. It is clearly seen in Table 3.3 that as water/solid ratio increases from 0.23 to 1.02, total pore volume of geopolymers increases from 0.0047 to 0.0138 cm^3/g and this leads to decrease in density of geopolymers. The highest total pore volume and lowest density is acquired for GP100M foamed geopolymer. Reduction in density as metakaolin proportion in samples increases might be due to the formation of open pores, which allow penetration of water and air [114].

Pore size distributions and densities of perlite-metakaolin based geopolymers are shown in Figure 3.11 and 3.12, respectively. Materials can be classified based on their pore sizes. Mesoporous materials contain pore diameters between 3.6-50 nm and macroporous materials include pore diameters between 50-200 nm [115]. Decomposition of hydrogen peroxide and geopolymerization of aluminosilicate raw materials directly affect pore size distribution of geopolymers. According to Figure 3.11, pore diameter distributions of GP80P20M, GP70P30M, GP60P40M and GP50P50M geopolymers are quite similar and in mesopore range. On the other hand, it can be interpreted from Figure 3.11 that pore diameter distribution of GP100P geopolymer is in macropore range. Evolution and coalescence of H_2 bubbles released by decomposition hydrogen peroxide is promoted in highly alkaline slurry; nevertheless, fast consolidation in the mixture results in broader pore size distribution [104] as in GP100P geopolymer. Rheology and amount of foaming agent should be optimized at the same time to control shape, distribution and coalescence of pores [104]. Pore size distribution of geopolymers is crucial for application area of them; for instance, insulation property is enhanced by narrow size distribution and acoustic resistance is empowered by wide pore size distribution [104, 116, 117].

Besides to all, the prominent result in Table 3.3 is BET surface area of GP80P20M geopolymer and it is measured as 16.5 m^2/g. It is known that zeolites have high surface area [118] and SEM image of GP80P20M depicts that zeolite A crystals are intensely found and this leads to high surface area for this specimen.

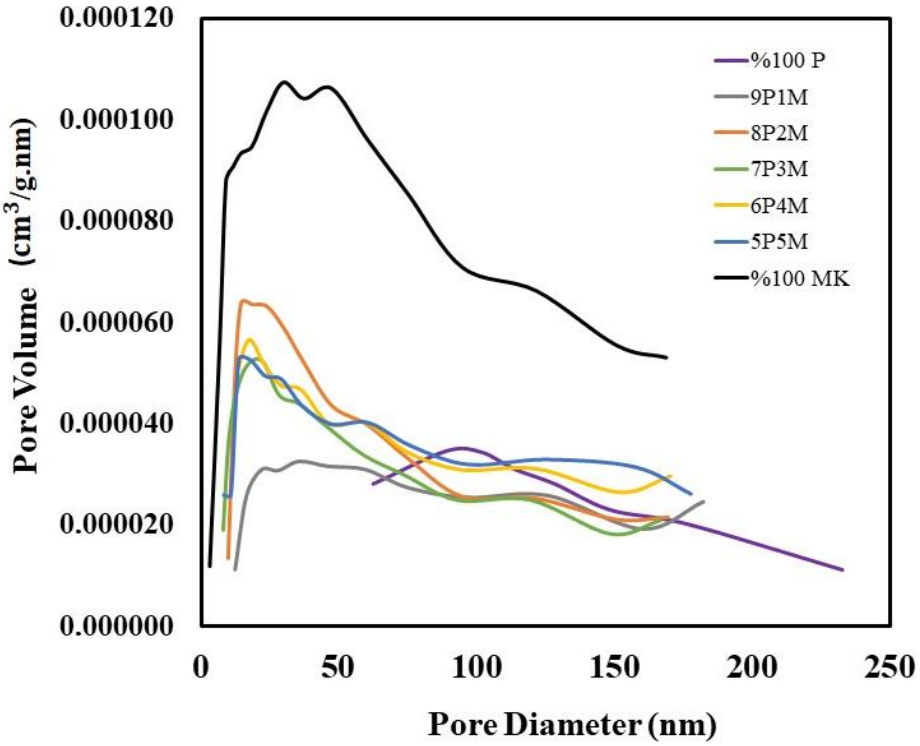

Figure 3.11. Pore size distributions of perlite-metakaolin based geopolymers determined by N_2 gas adsorption

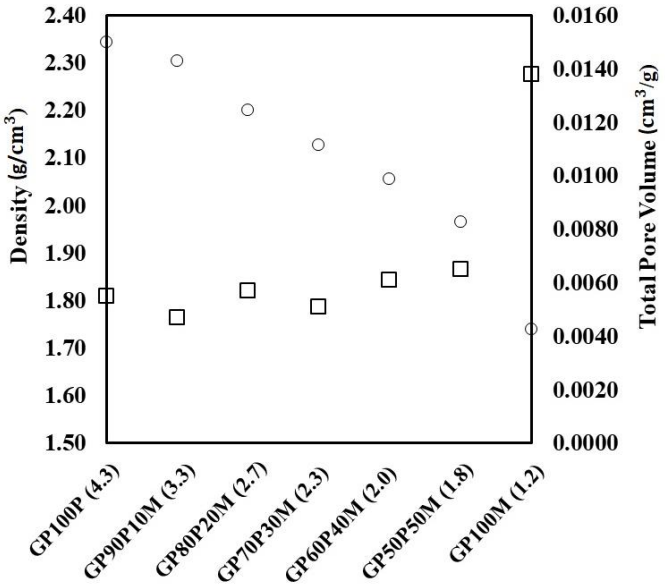

Figure 3.12. Density of perlite-metakaolin based geopolymers determined by water pycnometer (Si/Al molar ratios are specified in parentheses)

Figure 3.13 illustrates thermogravimetry curves of perlite-metakaolin based geopolymers. According to the TG curves, the most of the weight loss is observed before 200°C and between 200-700°C. Up to 200°C, the weight loss of geopolymers range between 2.77-12.2% and this loss is attributed to removal of free or interstitial water present in the structures of geopolymers [119, 120]. This result is confirmed by DSC thermograms of geopolymers presented in Figure 3.14. In Figure 3.14, it is seen that each DSC thermograms of geopolymers has an endothermic peak around 70 °C and the second peak is also observed around 100°C and 120°C for GP100P and GP100M geopolymers, respectively. These peaks detected in DSC thermograms are related to evaporation of free or chemically bond water from geopolymer network [120]. Moreover, TG curves depicts that weight loss between 200-700°C changes in the range of 3.8-4.8 % and this loss accounts for water which is strongly bound and less able to diffuse to the surface [119]. In the last section of TG curves, 700-1000 °C, the change in weight loss gets smaller with respect to the other sections; in other words, 0.39-1.20% weight loss observed and geopolymers are almost stable between 700-1000 °C. These small variations are attributed to densification of matrices due to crystallization [119]. These results are consistent with Table 3.3 that GP100M has the highest total pore volume hence it has the greatest weight loss and endothermic phase. GP100P geopolymer, on the other hand, has the smallest weight loss since its total pore volume is the smallest.

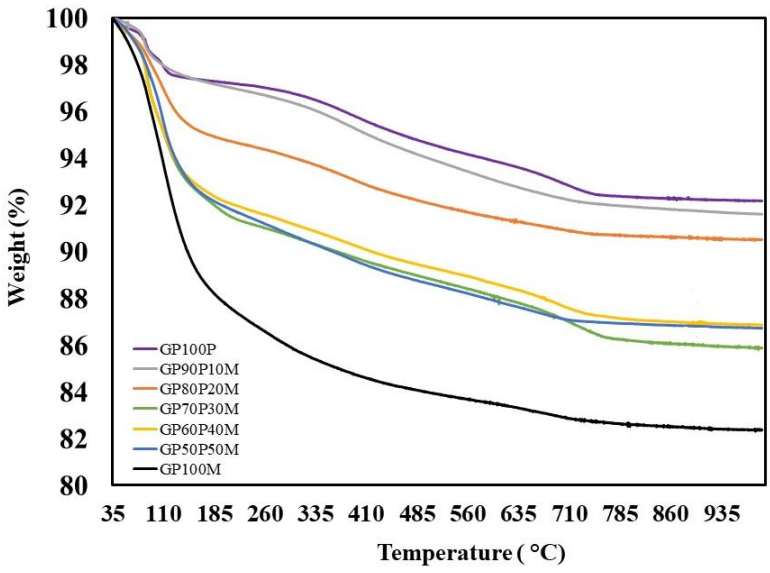

Figure 3.13: Thermal Gravimetric Analysis (TGA) of geopolymers

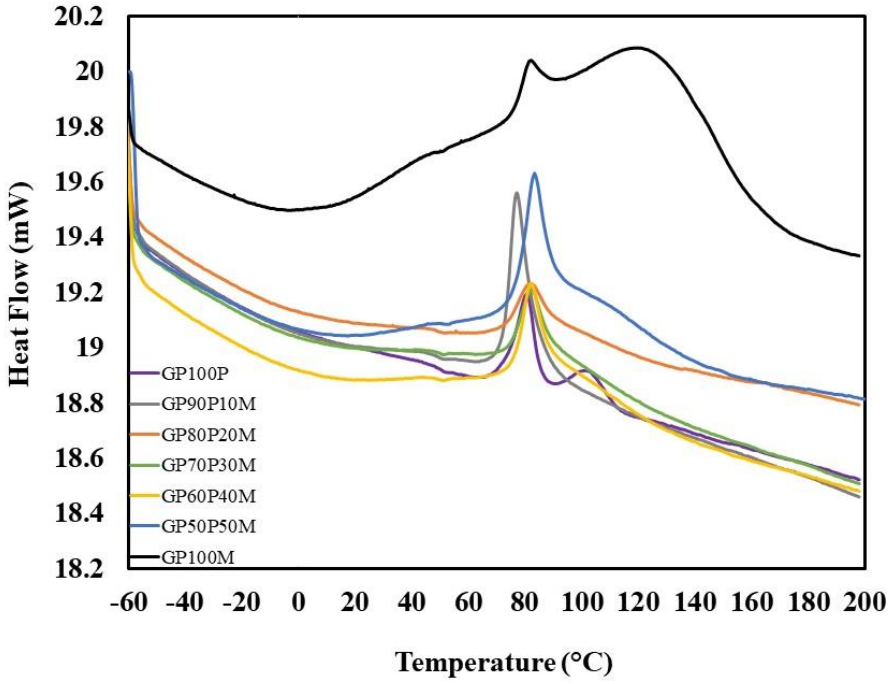

Figure 3.14: Differential Scanning Calorimetry (DSC) analysis of geopolymers

3.4. Conclusion

In this study, perlite-metakaolin based foamed geopolymers are synthesized with varying metakaolin contents of 0, 10, 20, 30, 40, 50, 100 wt% in raw material. The corresponding molar Si/Al ratios range from 4.3 to 1.2 and molar Na/Al ratio is kept constant at 1 for all specimens. The geopolymers are foamed with hydrogen peroxide. XRD, FTIR spectroscopy, SEM, BET, TGA/DSC analysis and density measurements are conducted to evaluate structural, thermal and physical characteristics of foamed geopolymers. XRD diffractograms demonstrate that zeolite phases emerge in geopolymers including 20% (wt.) and higher proportions of metakaolin whereas zeolite formation is suppressed in geopolymers with high Si/Al molar ratio (GP100P and GP90P10M). Besides, as metakaolin percentage increases in the system (and as molar Si/Al decreases) the broad feature centered around 23° in the XRD patterns shift to the higher angles (~27-29°) and this shift is correlated with formation of 3-D aluminosilicate structure. Structural changes within geopolymers are analyzed by means of FTIR spectroscopy and it is found that main absorption band shifts to lower frequencies (990-957 cm^{-1}) with the alteration in the local environment of Si-O bonds during geopolymerization reactions.

SEM results verify formation of cubic zeolite A in samples with lower Si/Al ratios. BET analysis and density measurements affirm each other such that as total pore volume of geopolymers increases the corresponding densities decrease. The highest total pore volume and the lowest density are measured for GP100M geopolymer as 0.0138 cm^3/g and 1.739 g/cm^3, respectively. As total pore volume increases, thermal stability of geopolymers decrease.

4. CONCLUSIONS AND RECOMMENDATIONS

4.1. Conclusions

The main objectives of this thesis are to investigate structure-performance relations in *one-part* volcanic ash based geopolymer systems and to obtain relationship between structural characteristics, physical and thermal properties of foamed perlite-metakaolin based geopolymers. Synthesized volcanic ash based *one-part* geopolymer specimens are analyzed by means of XRD, FTIR, SEM/EDS and compressive strength measurements; and perlite-metakaolin based foamed geopolymers are analyzed by XRD, FTIR, SEM, TGA/DSC, BET and together with density measurements.

In the first section of thesis, varying molar Si/Al and Na/Al ratios ranging between 2.5-4.5 and 1.1-5.1, respectively, are used to synthesize volcanic ash based *one-part* geopolymers. XRD analysis indicated that geopolymer structures consist of X-ray amorphous glassy network together with undissolved crystalline phases (mainly hematite, maghemite) embedded in the amorphous matrix. SEM images of the specimens display mostly homogenized glassy matrices. The main absorption band in the FTIR spectra indicating asymmetric stretching vibrations of Si-O-T bonds (T: Si, Al) in the geopolymeric framework constantly shifts to lower frequencies with increasing Si/Al and Na/Al molar ratios. The compressive strength values of one part geopolymers ascend with increasing Si/Al molar ratio and the highest compressive strength value attained in this study is 19.6 MPa.

In the second section of thesis, perlite-metakaolin based foamed geopolymers are synthesized with varying molar ratio of Si/Al and constant Na/Al, 1.2-4.3 and 1.0, respectively, in which hydrogen peroxide (3% wt.) is used as foaming agent. It is found in XRD analysis that as metakaolin amount in specimen increases or as Si/Al molar ratio decreases, the halo peak centered on 2θ region of 23° shifts to higher angles which is accepted as indication of geopolymerization.

Beside to this, zeolite A formation is observed for specimens containing at least 20% (wt) metakaolin and this formation also verified with SEM images. Increase in total pore volume of perlite-metakaolin based foamed geopolymers leads to decrease in densities of specimens according to the results of BET analysis and density measurements. Total pore volumes and densities range between 0.0047 to 0.0138 cm^3/g and 2.343 to 1.739 g/cm^3, respectively. The highest total pore volume results in the lowest thermal stability or vice versa.

4.2. Recommendations

Followings can be recommended for future studies:

Volcanic ash based *one-part* geopolymers can be synthesized with a broad range of molar Si/Al ratio to determine breakpoint of compressive strength; namely, the maximum compressive strength achievable for volcanic ash based *one-part* geopolymers, and to specify optimum molar Si/Al ratio in terms of compressive strength.

Mass spectra and ^{57}Fe Mössbauer spectra of volcanic ash based *one-part* geopolymers can be performed to investigate iron inclusion in detailed for *one-part* geopolymers.

Perlite-metakaolin based foamed geopolymers can be synthesized by means of *one-part* geopolymerization methods and structure-property relationships of geopolymers can be analyzed and compared to the specimens synthesized with conventional methods.

Sodium silicate solution can be utilized in the synthesis of perlite-metakaolin based foamed geopolymers as stabilizer that decreases the decomposition rate of hydrogen peroxide and decelerates the reaction.

Compressive strength of perlite-metakaolin based foamed geopolymers can be measured. Besides, a predictive model using finite elemental analyses can be established to correlate the size distribution of pores with their compressive strengths.

REFERENCES

1. Duxson, P. and Provis, J., "Low CO2 concrete: Are we making any progress?", *Royal Australian Institute of Architects*, 2008.
2. Sakulich, A., "Reinforced geopolymer composites for enhanced material greenness and durability", *Sustainable Cities and Society*, pp. 195-210, 2011.
3. Hardjito, D., Wallah, S., Sumajouw, D. and Rangan, B., "Brief review of development of geopolymer concrete", *George Hoff Symposium: American Concrete Institute*, 2004.
4. Damtoft, J., Lukasik, J., Herfort, D., Sorrentino, D. and Gartner, E., "Sustainable development and climate change initiatives", *Cement and Concrete Research*, 38 (2), pp. 115-127, 2008.
5. Hendriks, C., Worrell, E., Jager, D., Blok, K. and Riemer, P., "Emission reduction of greenhouse gases from the cement industry", *7th international conference on greenhouse gas control technologies*, 2004.
6. Duxson, P., Provis, J., Lukey, C. and van Deventer, J., "The role of inorganic polymer technology in the development of green concrete", *Cement and Concrete Research*, 37, pp. 1590-1597, 2007.
7. Mucsi, G., Lakatos, J., Molnar, Z. and Szabo, R., "Development of geopolymer using industrial waste materials", *The 9th International Conference "Environmental Engineering"*, Vilnius, Lithuania, 2014.
8. Vickers, L., van Riessen, A. and Rickard, W., "Precursors and Additives for Geopolymer Synthesis", *Fire-Resistant Geopolymers*, Springer Singapore, 2015, pp. 17-37.
9. Bondar, D., Lynsdale, C., Milestone, N., Hassani, N. and Ramazanianpour, A., "Effect of adding mineral additives to alkali-activated natural pozzolan paste", *Construction and Building Materials*, 25, 2906-2910, 2011.

10. Tchakoute, H.K., Elimbi, A., Mbey, J.A., Sabouang, C.J.N., Njopwouo, D., "The effect of adding alumina-oxide to metakalolin and volcanic ash on geoplymer products: A comparative study", *Construction and Building Materials,* 35, pp. 960-969, 2012.
11. Hossain, K., "Volcanic ash and pumice as cement additives: pozzolanic, alkali-silica reaction and autoclave expansion characteristics", *Cement and Concrete Research,* 35, pp. 1141-1144, 2005.
12. Lemougna, P.N., MacKenzie, J.D.K., Chinje Melo, U.F., "Synthesis and thermal properties of inorganic polymers (geopolymers) for structural and refractory applications from volcanic ash", *Ceramics International,* 37, pp. 3011-3018, 2011.
13. Tchakoute, H.K., Elimbi, A., Yanne, E., Djangang, C.N., "Utilization of volcanic ashes for the production of geopolymers cured at ambient temperature", *Cement & Concrete Composites,* 38, pp. 75-81, 2013.
14. Leonelli, C., Kamseu, E., Boccеccini, D., Melo, U., Rizzuti, A., Biilong, N. and Misselli, P., "Volcanic ash as alternative raw materials for traditional vitrified ceramic products", *Advanced Applied Ceramics,* 106, 2007.
15. Erdoğan, S., "Properties of Ground Perlite Geopolymer Mortars", *Journal of Materials Civil Engineering,* 27 (7), 2015.
16. Çelik, A., Kılıç, A. and Çakal, G., "Expanded Perlite Aggregate Characterization for Use as a Lightweight Construction Raw Material", *Physicochemical Problems of Mineral Processing,* 49 (2), pp. 689-700, 2013.
17. Benk, A. and Çoban, A. "Possibility of producing lightweight, heat insulating bricks from pumice and H3PO4-or NH4NO3- hardened molasses binder", *Ceramics International,* 38, pp. 2283-2293, 2012.
18. Şengül, O., Azizi, S., Karaosmanoglu, F. and Tasdemir, M., "Effect of expanded perlite on the mechanical properties and thermal conductivity of lightweight concrete", *Energy and Buildings,* 43, (2-3), pp. 671-676, 2011.
19. Doğan, M. and Alkan, M., "Some Physicochemical Properties of Perlite As An Adsorbent", *Fresenius Environmental Bulletin,* 13, pp. 252-257, 2004.

20. Tsaousi, G., Douni, I. and Panias, D., "Characterization of the properties of perlite geopolymer pastes", *Materiales de Construcción,* 66, 324, 2016.
21. USGS, *USGS Mineral Commodity Summaries, Perlite,* 2014, https://minerals.usgs.gov/minerals/pubs/mcs/2014/mcs2014.pdf, accessed at September 2017.
22. Kogel, J., Trivedi, N., Barker, J. and Krukowski, S., *Industrial Materials and Rocks-Commodities, Markets and Uses*, Society for Mining, Metallurgy and Exploration Inc.: Colorado, USA, 2006.
23. USGS, *Minerals Commodity Summaries*, 2016, https://minerals.usgs.gov/minerals/pubs/mcs/2016/mcs2016.pdf, accessed at September 2017.
24. Yazıcı, Ş. and İnan, G., "İnce agreganın bir kısmı yerine volkanik cüruf kullanımının beton özelliklerine etkisi", *Anadolu Üniversitesi Bilim ve Teknoloji Dergisi*, 6 (2), pp. 197-202, 2005.
25. Özer, I. and Soyer-Uzun, S., "Relations between the structural characteristics and compressive strength in metakaolin based geopolymers with different molar Si/Al ratios", *Ceramic International*, 41, pp. 10192-10198, 2015.
26. Newman, A., *Chemistry of clays and clay minerals*, Longman Scientific & Technical: New York, 1987.
27. Yip, K., Lukey, G., Provis, J. and van Deventer, J., "Effect of calcium silicate sources on geopolymerisation", *Cement and Concrete Research*, 38 (4), pp. 554-564, 2008.
28. Republic of Turkey Ministry of Economy, *Industry-Mining*, 2017. https://www.economy.gov.tr/portal/content/conn/UCM/uuid/dDocName:EK-021135, accessed at September 2017.
29. USGS, *Clays*, 2017. https://minerals.usgs.gov/minerals/pubs/commodity/clays/mcs-2017-clays.pdf, accessed at September 2017.
30. Yun-Ming, L., Cheng-Yong, H., Al Bakri, M. and Hussin, K., "Structure and properties of clay-based geopolymer cements: A review", *Progress in Material Science*, 83, pp. 595-629, 2016.

31. Bondar, D., Lynsdale, C., Milestone, N., Hassani, N. and Ramezanianpour, A., "Effect of type, form, and dosage of activators on strength of alkali-activated natural pozzolans", *Cement & Concrete Composites*, 33, pp. 251-260, 2011.

32. Duxson, P., Fernandez-Jimenez, A., Provis, J., Lukey, C., Palomo, A. and van Deventer, J., "Geopolymer technology: the current state of the art", *Journal of Material Science*, 42 (9), pp. 2917-2933, 2007.

33. van Jaarsveld, J., van Deventer, J. and Lukey, G., "The characterization of source materials in fly ash-based geopolmers", *Materials Letters*, 57, pp. 1272-1280, 2003.

34. Xu, H. and van Deventer, J., "The effect of alkali metals on the formation of geopolymeric gels from alkali-feldspars", *Colloids and Surfaces A: Physicochemical and Engineering Aspects*, 216 (1-3), pp. 27-44, 2003.

35. Davidovits, J., "Properties of Geopolymer Cements", *First international conference on alkaline cements and concretes*, Kiev, Ukraine, 1994.

36. Zuhua, Z., Xiao, Y., Haujun, Z. and Yue, J., "Role of water in the synthesis of calcined kaolin-based geopolymer", *Applied Clay Science*, 43 (2), pp. 218-223, 2009.

37. Juenger, M., Winnefield, F., Provis, J. and Ideker, J., "Advances in alternative cementitious binders", *Cement and Concrete Research*, 41 (12), pp. 1232-1243, 2011.

38. Provis, J., Activating Solution Chemistry for Geopolymers, *Geopolymers: Structures, Processing, Properties and Industrial Applications*, Cambridge, UK, 2009, pp. 50-71.

39. Criado, M., Fernández-Jiménez, A., DeLaTorre, A. and Aranda, M., "An XRD study of the effect of the SiO2/Na2O ratio on the alkali activation of fly ash", *Cement and Concrete Research*, 37 (5), pp. 671-679, 2007.

40. Nematollahi, B., Sanjayan, J. and Shaikh, F., "Synthesis of heat and ambient cured one-part geopolymer mixes with different grades of sodium silicate", *Ceramics International*, 41, pp. 5696-5704, 2015.

41. Najafi Kani, E., Allahverdi, A. and Provis, J., "Effloresence geopolymer binders based on natural pozzolan", *Cement and Concrete Composites*, 34 (1), pp. 25-33, 2012.

42. Feng, D., Provis, J. and van Deventer, J., "Thermal activation of albite for the synthesis of one part mix geopolymers", *Journal of American Ceramic Society*, 92 (2), pp. 565-572, 2012.

43. Koloušek, D., Brus, J., Urbanova, M., Andertova, J. and Hulin, V., "Preparation, structure and hydrotherma lstability of alternative (sodium silicate free) geopolymers", *Journal of Material Science,* 42 (22), pp. 9267-9275, 2007.

44. Hajimohammadi, A., Provis, J. and van Deventer, J., "Effect of Alumina Release Rate on the Mechanism of Geopolymer Gel Formation", *Chemistry of Materials,* 22 (18), pp. 5199-5208, 2010.

45. Ke, X., Bernal, S., Ye, N., Provis, J. and Yang, J., "One-Part geopolymers based on thermally treated red mud/NaOH blends", *Journal of American Ceramic Society,* 98 (1), pp. 5-11, 2015.

46. Duxson, P. and Provis, J., "Designing precursors for geopolymer cements", *Journal of American Ceramic Society,* 91 (12), pp. 3864-3869, 2008.

47. Davidovits, J., "Geopolymers: inorganic polymeric new materials", *Journal of Material Education*, 16, pp. 91-139, 1994.

48. Rovnanik, P., "Effect of curing temperature on the development of hard structure of metakaolin-based geopolymer", *Construction and Building Materials,* 24 (7), pp. 1176-1183, 2010.

49. Lizcano, M., Kim, H., Basu, S. and Radovic, M., "Mechanical properties of sodium and potassium activated metakaolin-based geopolymers", *Journal of Materials Science,* 47 (6), pp. 2607–2616, 2012.

50. Davidovits, J., "Geopolymer chemistry and properties", *Proceedings of the 1st International Conference on Geopolymer*, Compiegne, France, 1988.

51. Davitovits, J., "High-Alkali Cements for 21st Century Concretes", *American Concrete Institute,*144, pp. 383-398, 1994.

52. Vaou, V. and Panias, P., "Thermal insulating foamy geopolymers from perlite", *Minerals Engineering*, 23, pp. 1146-1151, 2010.

53. Comrie, D., Paterson, J. and Ritcey, D., "Geopolymer Technologies in Toxic Waste Management", *Proceedings of the 1st International Conference on Geopolymer*, Compiegne, France, 1988.

54. Davitovits, J., "Recent progresses in concretes for nuclear waste and uranium waste containment", *Concrete International,* 16 (12), pp. 53-58, 1994.

55. Davitovits, J., "Geopolymers: Inorganic polymeric new materials", *Journal of Thermal Analysis*, 37, pp. 1633-1656, 1991.

56. Davidovits, J., Buzzi, L., Rocher, P. and Gimeno, D., "Geopolymeric cement based on low cost geologic materials", *Proceedings of the 2nd International Conference on Geopolymer*, Saint Qunentin, France, 1999.

57. van Jaarsveld, J., *The physical and chemical characterisation of fly ash based geopolymers*, University of Melbourne, Australia, 2000.

58. Komnitsas, K. and Zaharaki, D., "Geopolymerisation: a review and prospects for minerals industry", *Mineral Engineering*, 20, pp. 1261-1277, 2007.

59. Davitovits, J. and Davidovics, M., "Geopolymer: Ultra-high temperature tooling material for the manufacture of advanced composites", *International SAMPE Symposium and Exhibition*, Saint Quentin, France, 1991.

60. Davitovits, J., "30 Years of Successes and Failures in Geopolymer Applications. Market Trends and Potential Breakthroughs", *Geopolymer 2002 Conference*, Melbourne, Australia, 2002.

61. Rowles, M. and O'Connor, B. "Chemical optimisation of the compressive strength of aluminosilicate geopolymers synthesised by sodium silicate activation of metakaolinite", *Journal of Materials Chemistry*, 5, pp. 1161-1165, 2003.

62. Heah, C., Kamarudin, H., Al Bakri, M., Bnhussain, M., Luqman, M., Khairul Nizar, I., Ruzaidi, C. and Liew, Y., "Study on solids-to-liquid and alkaline activator ratios on kaolin-based geopolymers", *Construction and Building Materials*, 35, pp. 912-922, 2012.

63. Provis, J., "Correlating mechanical and thermal properties of sodium silicate-fly ash geopolymers", *Colloids and Surfaces: A Physochemical and Engineering Aspects*, 336, pp. 57-63, 2009.

64. Xie, J. and Kayali, O., "Effect of initial water content and curing moisture conditions on the development of fly ash-based geopolymers in heat and ambient temperature", *Construction and Building Materials*, 67, pp. 20-28, 2014.

65. Lizcano, M., Gonzalez, A., Basu, S., Lozano, K. and Radovic, M., "Effects of Water Content and Chemical Composition on Structural Properties of Alkaline Activated Metakaolin-Based Geopolymers", *Journal of the American Ceramic Society*, 95 (7), pp. 2169–2177, 2012.

66. Rahier, E., Wastiels, J., Biesemans, M., Willem, R., van Assche, G. and van Mele, B., "Reaction mechanism, kinetics and high temperature transformations of geopolymers", *Journal of Materials Science,* 42 (9), pp. 2982–2996, 2007.

67. Arioz, E., Arioz, Ö. and Koçkar, Ö.M., "The Effect of Curing Conditions on the Properties of Geopolymer Samples", *International Journal of Chemical Engineering and Applications,* 4, pp.423-426, 2013.

68. Perera, D., Uchida, O., Vance, E. and Finnie, K., "Influence of curing schedule on the integrity of geopolymers", *Journal of Materials Science,* 42 (9), pp. 3099–3106, 2007.

69. Provis, J. and van Deventer, J., "Geopolymerization kinetics. 2. Reaction kinetic modelling", *Chemical Engineering Science,* 67, pp. 2318, 2007.

70. Hajimohammadi, A., Provis, J. and van Deventer, J., "One-Part geopolymer from geothermal silica and sodium aluminate", *Industrial Engineering and Chemistry Research,* 47, pp. 9396-9405, 2008.

71. Fernandez-Jimenez, A. and Puertas, F., "Effect of activator mix on hydration and strength behaviour of alkali activated slag cements", *Advanced Cement Research,* 15 (3), pp. 129-136, 2003.

72. Djobo, J., Elimbi, A., Tchakoute, H.K. and Kumar, S., "Volcanic ash-based geopolymer cements/concretes: the current state of the art and perspectives", *Environmental Science and Pollution Research,* 24 (5), pp. 4433-4446, 2017.

73. Tchakoute, H.K., Elimbi, A., Diffo Kenne, B., Mbey, J. and Njopeouo, D., "Synthesis of geopolymers from volcanic ash via the alkaline fusion method: Effect of Al_2O_3/Na_2O molar ratio of soda–volcanic ash", *Ceramics International,* 39 (1), pp. 269-276, 2013.

74. Djobo, J., Elimbi, A., Tchakoute, H.K. and Kumar, S., "Mechanical activation of volcanic ash for geopolymer synthesis: effect on reaction kinetics, gel characteristics, physical and mechanical properties", *RSC Advances,* 45 (6), pp. 39106-39117, 2016.

75. Provis, J., *Modelling the formation of geopolymers,* Australia: University of Melbourne, 2006.

76. Kaya, K. and Soyer-Uzun, S., "Evolution of structural characteristics and compressive strength in red mud-metakaolin based geopolymer systems", *Ceramics International,* 42, pp. 7406-7413, 2016.

77. Perera, D.S., Cashion, J.D., Blackford, G.M., Zhang, Z. and Vance, E.R., "Fe speciation in geoplymers with Si/Al molar ratio of 2", *Journal of European Ceramic Society,* 27, pp. 2697-2703, 2007.

78. Lemougna, P.N., MacKenzie, J.K., Jameson, N.G., Rahier, H. and Chinje Melo, U.F., "The role of iron in the formation of inorganic polymers (geopolymers) from volcanic ash: a ^{57}Fe Mössbauer spectroscopy study", *Journal of Material Science,* 48, pp. 5280-5286, 2013.

79. Yip, C. and van Deventer, J., "Effect of granulated blast furnace slag on geopolymerization", *6th World Congress of Chemical Engineering*, Melbourne, Australia, 2001.

80. Phair, J. and van Deventer, J., "Effect of silicate activator PH on the leaching and material characteristics of waste-based inorganic polymers", *Minerals Engineering,* 14 (3), pp. 289-304, 2001.

81. Villa, C., Pecina, E., Torres, R. and Gomez, L., "Geopolymer synthesis using alkaline activation of natural zeolite", *Construction and Building Materials,* 24 (11), pp. 2084-2090, 2010.

82. Fernandez-Jimenez, A. and Palomo, A., "Compostion and microstructure of alkali activated fly ash binder: effect of the activator", *Cement Concrete Research,* 35, pp. 1984-1992, 2005.

83. Takeda, H., Hashimoto, S., Kanie, H., Honda, S. and Iwamoto, Y., "Fabrication and characterization of hardened bodies form Japanese volcanic ash using geopolymerization", *Ceramics International,* 40, pp. 4071-4076, 2014.

84. Lee, W. and van Deventer, J., "Structural reorganisation of class F fly ash in alkaline silicate solution", *Collaidal Surface A,* 211, pp. 49-66, 2002.

85. Zhang, Y., Wei, S. and Zongjin, L., "Composition design and microstructural characterization of calcined kaolin-based geopolymer cement", *Applied Clay Science,* 47, pp. 271-275, 2010.

86. Duxson, P., Mallicoat, S., Lukey, G., Kriven, W. and van Deventer, J., "The effect of alkali and Si/Al ratio on the development of mechanical properties of metakaolin-based geopolymers", *Colloids and Surfaces A: Physicochemical and Engineering Aspects,* 292 (1), pp. 8-20, 2007.

87. Steveson, M. and Sagoe-Crentsil, K., "Relationships between composition, structure and strength of inorganic polymers", *Journal of Materials Science,* 40 (16), pp. 4247-4259, 2005.

88. Williams, R. and van Riessen, A., "Development of alkali activated borosilicate inorganic polymers (AABSIP)", *Journal of the European Ceramic Society,* 31 (8), pp. 1513-1516, 2011.

89. Hajimohammadi, A. and van Deventer, J., "Characterisation of One-Part Geopolymer Binders Made from Fly Ash", *Waste and Biomass Valorization,* 8 (1), pp. 225-233, 2017.

90. Wu, H. and Sun, P., "New building materials from fly ash-based lightweight inorganic polymer", *Construction and Building Materials,* 21, pp. 211-217, 2007.

91. Xu, H. and van Deventer, J., "Geopolymerisation of multiple minerals", *Minerals Engineering,* 15, pp. 1131-1139, 2002.

92. Zivica, V., Palou, M. and Krizma, M., "Geopolymer Cements ans Their Properties: A Review", *Building Research Journal,* 61 (2), pp. 85-100, 2014.

93. Rees, C., *Mechanisms and kinetics of gel formation in geopolymers,* Australia: The University of Melbourne, 2007.

94. Tsaousi, G.M., Douni, I., Taxiarchou, M., Panias, D. and Paspaliaris, I., "Development of foamed Inorganic Polymeric Materials based on Perlite", *3rd International Conference on Competitive Materials and Technology Processes,* 2016.

95. Holt, E. and Raivio, P., "Use of gasification residues in aerated autoclaved concrete", *Cement and Concrete Research,* 35, pp. 796-802, 2005.

96. Jerman, M., Keppert, M., Vyborny, J. and Cerny, R., "Hygric, thermal and durability properties of autoclaved aerated concrete", *Construction and Building Materials,* 41, pp. 352-359, 2013.

97. Kenne Diffo, B., Elimbi, A., Cyr, M., Dika Manga, J. and Kouamo, H., "Effect of the rate of calcination of kaolin on the properties of metakaolin-based geopolymers", *Journal of Asian Ceramic Societies,* 3 (1), pp. 130-138, 2015.

98. Vance, E., Perera, D., Imperia, P., Cassidy, D., Davis, J. and Gourley, T., "Perlite waste a a precurser for geopolymer formation", *Journal of the Australian Ceramic Society,* 45 (1), pp. 44-49, 2009.

99. Tangkawanit, S. *Synthesis of zeolites from perlite and study of their ion exchange properties,* Nakhon Ratchasima, Thailand: Suranaree University of Technology, 2004.

100. He, J., Zhang, J., Yu, Y. and Zhang, G., "The strength and microstructure of two geopolymers derived from metakaolin and red mud-fly ash admixture: A comparative study", *Construction and Building Materials,* 30, pp. 80-91, 2012.

101. Rees, C., Provis, J., Lukey, G. and van Deventer, J., "In situ ATR-FTIR study of the early stages of fly ash geopolymer gel formation", *Langmuir,* 23, pp. 9076-9082, 2007.

102. Hajimohammadi, A., Ngo, T., Mendis, P., Nguyen, T., Kashani, A. and van Deventer, J., "Pore characteristics in one-part mix geopolymers foamed by H_2O_2: The impact of mix design", *Materials & Design,* 130, pp. 381-391, 2017.

103. Langille, K., Nguyen, D., Bernt, J. and Veinot, D., "Mechanism of dehydration and intumescence of soluble silicates Part II: effect of the cation", *Journal of Material Science,* 26, pp. 704-710, 1991.

104. Papa, E., Medri, V., Kpogbemabou, D., Morinière, V., Laumonier, J., Vaccari, A. and Rossignol, S., "Porosity and insulating properties of silica-fume based foams", *Energy and Buildings,* 131, pp. 223-232, 2016.

105. Provis, J. and van Deventer, J., Accelerated aging of geopolymers, *Geopolymers Structure, Processing, Properties and Industrial Applications*, Cambridge, UK, Woodhead Publishing , 2009, pp. 145-163.

106. Davitovits, J., "Structural characterization of geopolymeric materials with X-ray diffractometry and MAS-NMR spectrometry", *Geopolymere '88,* pp. 149-166, 1988.

107. Criado, M., Fernandez Jimenez, A., Sobrados, I., Palomo, A. and Sanz, J., "Effect of relative humidity on the reaction products of alkali activated fly ash", *Journal of European Ceramic Society,* 32 (11), pp. 2799-2807, 2012.

108. Barbosa, V., MacKenzie, K. and Thaumaturgo, C., "Synthesis and characterization of materials based on inorganic polymers of alumina and silica: Sodium polysialate polymers", *International Journal Inorganic Materials,* 2 (4), pp. 309-317, 2000.

109. Davidovits, J., *Geopolymer Chemistry and Applications*, Institut Géopolymère, St.Quentin, France , 2008.

110. Fernandes, I., Noronha, F. and Teles, M., "Microscopic analysis of alkali–aggregate reaction products in a 50-year-old concrete", *Materials Characterization,* 53, pp. 295-306, 2004.

111. Gouloure, Z., Nait-Ali, B., Zekeng, S. and Kams, E., "Recycled natural wastes in metakaolin based porous geopolymersfor insulating applications", *Journal of Building Engineering,* 3, pp. 58-69, 2015.

112. Kamseu, E., Goulore, Z., Nait Ali, B. and Zeken, S., "Cumulative pore volume, pore size distribution and phasespercolation in porous inorganic polymer composites: relation microstructure and effective thermal conductivity", *Energy Buildings,* 88, pp. 45-56, 2015.

113. Zhang, Z., Yao, X. and Zhu, H., "Potential application of geopolymers as protection coatings for marine concrete: II. Microstructure and anticorrosion mechanism", *Applied Clay Science,* 49, pp. 7-12, 2010.

114. Risdanareni, P., Puspitasari, P., Santos, E. and Prasetya Adi, E., "Mechanical and physical properties of metakaolin based geopolymer paste", *MATEC Web of Conferences*, 2017.

115. Kramar, S. and Ducman, V., "Mechanical and microstructural characterization of geopolymer synthesized from low calcium fly ash", *Chemical Industry & Chemical Engineering Quarterly*, 21 (1), pp. 13-22, 2015.

116. Feng, J., Zhang, R., Gong, L., Li, Y., Cao, W. and Cheng, X., "Development of porous fly ash base geopolymer with low thermal conductivity", *Materials and Design,* 65, pp. 529-533, 2015.

117. Han, F., Seiffert, G., Zhao, Y. and Gibbs, B., "Acoustic absorption behaivour of an open celled aluminum foam", *Journal of Physical D Applied Physics,* 36 (3), pp. 294, 2003.

118. Yates, D., "Studies on surface area of zeolites, as determined by physical adsorption and X-ray crystallography", *Canadian Journal of Chemistry,* 46, pp. 1965-1701, 1968.

119. Zhang, H., Kodur, V., Wu, B., Cao, L. and Wang, F., "Thermal behavior and mechanical properties of geopolymer mortar after exposure to elevated temperatures", *Construction and Building Materials,* 109, pp. 17-24, 2016.

120. Kaddoussi, I., Baklouti, S., Arous, M. and Fakhfakh, Z., "Water molecular dynamics of metakaolin and phosphoric acid-based geopolymers investigated by impedance spectroscopy and DSC/TGA", *Journal of Non-Crystalline Solids,* 445-446, pp. 95-101, 2016.